Large Eddy Simulations of flow around tandem circular cylinders in the vicinity of a plane wall

Mia Abrahamsen Prsic, Muk Chen Ong[#], Bjørnar Pettersen*, Dag Myrhaug**

** Department of Marine Technology, Norwegian University of Science and Technology, NO-7491 Trondheim, Norway*
[#] Department of Mechanical and Structural Engineering and Materials Science, University of Stavanger, NO-4036 Stavanger, Norway

Abstract

In order to investigate the three-dimensional flow around free-spanning, tandem marine pipelines, Large Eddy Simulations (LES) with Smagorinsky subgrid scale model are performed using the open-source code OpenFOAM. Two circular cylinders in tandem arrangement are placed in the vicinity of a rigid, horizontal, plane wall. The cylinders are immersed in a steady current with a logarithmic boundary layer profile at an intermediate, subcritical Reynolds number ($Re = 1.31 \times 10^4$). The non-dimensional distances between the cylinder centres are 2 and 5 (L/D = 2 and 5) and the gap to diameter ratios are G/D = 0.6 and 1, where gap G is the distance between the bottom of the cylinders and the wall.

The present results are analysed through the values of drag and lift coefficients, as well as by the details of the flow fields in the wake of the cylinders. The results are compared with experimental results of the flow around tandem cylinders in an unlimited fluid for both L/D = 2 and 5, showing that, at chosen gaps, at L/D = 2, the flow belongs to the reattachment regime, and at L/D = 5 to the co-shedding regime. Compared with the case of a single cylinder near a plane wall, the flow around the tandem cylinders at G/D = 1 belongs to the wide gap regime, while at G/D = 0.6, tandem yields a stronger interaction with the wall than in the case of one cylinder. The presence of the wall modifies the flow in the spacing between the two cylinders, giving it some characteristics of the extended body flow regime.

KEY WORDS: tandem circular cylinders; wall proximity; Large Eddy Simulations; wake flow, OpenFOAM.

1. Introduction

Circular cylinders are commonly used in engineering structures, appearing single or in bundles, isolated or in interaction with other objects. Subsea pipelines, marine risers and columns of platform legs are only some examples in the current driven marine environment, while chimneys, power lines and cables represent cylindrical structures exposed to the air flow. The key parameter in this type of flow is the Reynolds number, $Re = U_c D/\upsilon$, where U_c is the free stream velocity, D is the cylinder diameter and υ is the kinematic viscosity of the fluid. Classification of the flow regimes around a smooth, circular cylinder in steady, uniform flow with respect to Re was presented in [1], ranging from a laminar flow

with two fixed, symmetric wake vortices, to a fully developed vortex street with both turbulent wake and turbulent boundary layer.

Due to the wide spread of engineering applications; the flow around a single circular cylinder immersed in an unlimited fluid is a well explored fluid flow topic. Comprehensive reviews of both the physical phenomenon and the previously published results were given in [1] and [2]. Detailed experimental results span from the measurements done almost a century ago [3] to the modern Particle Image Velocimetry (PIV) measurements, allowing an insight on the turbulence statistics in the nearest wake of the cylinder [4]. Many in-depth studies were also published in the field of Computational Fluid Dynamics (CFD), for various Re range. To name some of the recent three-dimensional studies, Large Eddy Simulations (LES) results were presented by Krajnovic [5], Lysenko et al. [6], Abrahamsen Prsic et al. [7, 8] and Direct Numerical Simulations (DNS) by Tremblay et al. [9].

In all of the previously mentioned structures, circular cylinders often appear in pairs or bundles. In the simplest case, the two cylinders of same diameter are placed in a tandem formation and exposed to a uniform incoming current in otherwise unlimited fluid. The physical behaviour of the flow is complex, involving an interaction between the von Karman vortex streets, the cylinder wakes and the shear layers. Re is again an important parameter, resulting in laminar or turbulent vortex streets and boundary layers on the upstream cylinder. The presence of the downstream cylinder has, however, a dramatic influence on the flow behaviour around both cylinders. Based on the normalized distance between the tandem cylinders centres (L/D, also called the spacing ratio) and Re, Zdravkovich [10] classified several different flow regimes. Three main regimes were referred to as the extended body, the reattachment and the co-shedding regime, while the second step of classification divides the interference flow regimes in the subcritical, critical and post-critical states [11]. Considering the subcritical state, used in the present study, the relatively large L/D in the co-shedding regime allows vortex shedding from both cylinders, while small L/D of the first two regimes suppresses the shedding from the upstream cylinder.

Although less explored than the flow around a single cylinder, the flow around the two-cylinder configurations recently received significant attention. Extensive experimental studies were conducted in attempts to classify the flow types around the tandem cylinders. Zdravkovich and Pridden [12] documented the discontinuities in the base pressure and the drag and the lift forces exerted on the downstream cylinder due to changes in flow patterns around the tandem cylinders with changing L/D. Zdravkovich [13] dedicated a large chapter of the book on flow around cylinders to a comprehensive categorisation of the flow patterns at various L/D. Lin et al. [14] focused on the details of instantaneous and averaged velocity fields, observed by PIV. Alam et al. [15] carried out a systematic analysis of the subcritical flow regime, presenting the variations in the fluctuating fluid forces for L/D between 1 and 7 (with small increments) in order to capture the discontinuities. Zhou and Yiu [16] performed experiments at Re = 7000 and discovered large differences in flow structures depending on the position where the shear layers from the upstream cylinder reattach on the downstream cylinder. Song et al. [17] reported about the narrow and the wide gap flow in the wake of the two side by side cylinders at Re range between 1000 and 5000, utilizing PIV. Most of the studies were conducted for the sub-critical Re, ranging from 1×10^4 to 8×10^4. A detailed review of the experimental results, including both the classic and various modern measurements was published by Sumner [18], who summarised the current understanding of the flow around long circular cylinders of equal diameter, exposed to steady cross-flow. Focus was on the near-wake flow patterns, the intermediate wake behaviour and variability with respect to Re.

The complexity of the flow around the tandem cylinders implies high demands on the computational resources. The previously published results were therefore often limited to 2D

simulations at low Re. To name some: Mittal et al. [19] employed a finite element formulation to simulate flow around tandem cylinders at L/D = 2.5 and 5.5 for Re = 100 and 1000, and Meneghini et al. [20] presenting detailed vorticity calculations and wake flow visualisation for Re = 100 and 200.

Recently, the development of both more sophisticated numerical methods and the supercomputers enabled fast progress in the research on the higher Re number flow. Lattice Boltzmann method was utilized in [21] to model the flow around tandem cylinders at L/D = 3.7 and Re = 1.66 x 10^5, comparing the simulations with the periodic boundary conditions to the ones with finite cylinder length and vertical side plates (no slip boundary condition). At comparable Re number, several studies were conducted using various types of LES. In [22] standard LES with Smagorinsky subgrid scale model is utilized, the same as in the present study, at comparable Re = 2.2 x 10^4, to explore the characteristics of the vortices shed from the circular tandem cylinders at L/D = 2 and 5. In [23] Delayed Detached Eddy Simulations (DDES) were used, and in [24], the variational multi-scale and the classic LES with Smagorinsky subgrid scale model, to simulate the flow around tandem circular cylinders at L/D = 3.7 and Re = 1.66 x 10^5. Tandem of square cylinders was discussed in [25].

A simple example of a free-spanning subsea pipeline points towards another parameter influencing the flow around circular cylinders – the vicinity of the sea bed or other types of constraints. In the case of a single circular cylinder placed near a plane wall with a gap G between the pipeline and the wall, the key parameter is the gap to diameter ratio, G/D. The profile of the wall boundary layer of the incoming flow is also important, [26]. Proximity to the plane wall affects the flow around the cylinder and its wake, resulting in two main flow regimes. In the narrow gap flow regime, the vortex shedding is suppressed, the wake flow is reattached to the plane wall, and the cylinder wake is asymmetric. As G/D exceeds the critical value of about 0.3 [1], von Karman vortices begin to form in the cylinder wake and the bottom wall boundary layer experiences periodic shedding. Moving the cylinder farther from the wall results in gradual re-establishment of the wake symmetry. At G/D > 2, the influence of the wall subsides and the flow obtains the characteristics of the cylinder in the infinite fluid case [13].

Experimental measurements were performed for both low, Re < 300, and intermediate subcritical, Re < 3 x 10^5 (for the comprehensive overview over previously published measurements, see [26]). Along with the traditional point measurements, PIV offers a good insight into the flow structures in the cylinder wake. For the subcritical Re range, measurements were published by Price et al. [27], Alper Oner et al. [28] and Wang and Tan [29]. Numerical studies were mainly limited to 2D simulations using the Reynolds-Averaged Navier-Stokes (RANS) models. RANS results presented by Brørs [30] at Re = 1.5 x 10^4, Zhao et al. [31] at Re = 9 x 10^3 and Ong et al. [32] at Re = 1.31 x 10^4 offered a reasonable qualitative agreement with the experiments, but showed limitations due to the incapability of capturing the three-dimensionality of the flow or the specific features of the flow at certain G/D. LES simulations at lower Re = 1.44 x 10^3 [33] and intermediate Re = 1.31 x 10^4 [26] gave an insight into the 3D wake and the behaviour of the vortices.

Even though the previously mentioned physical configurations tend to be analysed separately, the complexity of the engineering structures often utilizes a combination of more than one circular cylinder in the close vicinity of a wall. This topic has, however, received very little attention. Recently, the influence of the wall proximity on the flow around tandem cylinders was experimentally explored by Wang et al. [34]. Using PIV and measurements of fluid dynamic forces, they measured the flow around the tandem cylinders at G/D ranging from 0.15 to 2 and L/D between 1.5 and 6, at subcritical Re = 6.3 x 10^3, focusing on the flow force coefficients and wake velocity fields. Bhattacharyya and Dhinakaran [35] and Harichandan and Roy [36] published the numerical studies of the flow around tandem square cylinders in the vicinity of a plane wall at very low Re = 100 and 200. Zhao et al. [37] used RANS to simulate the scour around tandem pipelines laid on the erodible, sandy seabed. They

focused on the enlarged scour behind the downstream cylinder, obtaining results comparable to the experimental studies. Li et al. [38] presented LES of flow around tandem circular cylinders near a plane wall at small gap to diameter ratio, discussing the hydrodynamic flow coefficients as well as the alterations of the flow fields due to the immediate vicinity of the wall. Abrahamsen Prsic et al. [8] performed LES around tandem circular cylinders in the wide gap regime (G/D = 1) at the same Re = 1.31 x 10^4 as in the present study. For L/D = 2 and 5, the results were compared to the flow around a single cylinder at G/D = 1 from the plane wall. Time histories of the drag and the lift coefficient as well as instantaneous and averaged values of the vorticity and the velocity fields in the cylinder wake were used to depict general characteristics of the flow.

The configuration of tandem cylinders in the vicinity of a plane wall, though, appears often in the offshore technology, for example as double free-spanning subsea pipelines. Therefore the present paper focuses on the flow around two tandem circular cylinders in the vicinity of a plane wall, at various spacing and gap ratios. Re = 1.31 x 10^4 belongs to the intermediate, subcritical Re range and is chosen to correspond to the operational conditions of near-bottom pipelines. In the North Sea, at the water depth of about 100 m, the pipelines are on average exposed to relatively slow current, between 0.02 m/s and 0.5 m/s [39]. The diameter of a pipeline can vary in size from as much as 1.066 m (44 inch), through commonly used 0.76 m (30 inch) and 0.404 m (16 inch) to as small as 0.05 m (2 inch) [40]. The chosen Re thus covers a variety of combinations a real offshore pipeline or marine riser can experience.

Based on the published numerical research for both the single circular cylinder in the vicinity of the wall and two tandem cylinders in a uniform flow, LES has proven to be a good numerical tool for the analysis of these problems. The detailed examination of the instantaneous flow properties through the drag and the lift force, vorticity and Q criterion showed that LES provides an insight in the temporal development of the wake flow and the interaction between the wakes of the two cylinders [8]. The time-averaged values, obtained through simulations of the fully developed flow (with data sampled after the quasi-steady state is accomplished) over many vortex shedding periods, allow the discussion about the overall details of the physical phenomena. The criteria for determining whether the flow is fully developed, used in this study are described in [41].

The flow is governed by two key parameters – the spacing ratio (L/D) and the gap ratio (G/D). In this study, L/D = 2 and 5. The larger spacing ratio is chosen as a clear representation of the co-shedding regime, while L/D = 2 results in wake proximity interference [11], and was previously classified in both the extended body and the reattachment flow regime (for the case of tandem cylinders in an infinite fluid).

The cylinders are placed 0.6D and 1D from a plane wall. Previously published results of flow around a single cylinder in the vicinity of a plane wall [26] indicated that at G/D = 1, the interaction between the wall flow and the cylinder wake still exists. The effects on the cylinder wake are, however, mild, allowing the present results, at G/D = 1, to be compared to those of the tandem cylinders in an infinite fluid. At G/D = 0.6, on the other hand, the cylinders are placed under stronger influence of the wall, allowing the complex interaction between the cylinder wakes and the wall boundary layer to develop. Considering the relatively large spacing, L/D = 5, the flow around each cylinder in tandem is compared to the case of a single cylinder in the vicinity of the wall.

2. *Numerical method and computational set-up*

2.1. Governing equations

In the present study, LES of the incompressible flow are performed with the Smagorinsky subgrid-scale model. The incompressible Navier-Stokes equations and the momentum equation in the filtered form (i.e. after elimination of subgrid scales), can be written as:

$$\frac{\partial \overline{u}_i}{\partial x_i} = 0 \tag{1}$$

$$\frac{\partial \overline{u}_i}{\partial t} + \frac{\partial \left(\overline{u}_i \overline{u}_j \right)}{\partial x_j} = -\frac{1}{\rho} \frac{\partial \overline{p}}{\partial x_i} + \nu \frac{\partial^2 \overline{u}_i}{\partial {x_j}^2} - \frac{\partial \tau_{ij}}{\partial x_j} \tag{2}$$

where $\overline{u_i}$, i ∈ [1, 2, 3] denotes the filtered velocity component in streamwise (x), crossflow (y) and spanwise (z) direction, respectively (see Figure 1) x_i is assigned to the respective directions, ρ is the density of the fluid, $\overline{p}$ is the filtered pressure and τ_{ij} represents the non-resolvable subgrid stress, given by:

$$\tau_{ij} = \overline{u_i u_j} - \overline{u}_i \overline{u}_j \tag{3}$$

The commonly used subgrid scale model proposed by Smagorinsky [42] is used in the present study to include the effect of the subgrid scale motions. Through Boussinesq approximation, introducing the turbulent eddy viscosity ν_t, the subgrid stress is given as:

$$\tau_{ij} - \frac{1}{3}\delta_{ij}\tau_{kk} = -2\nu_t \overline{S}_{ij} \tag{4}$$

$$\overline{S}_{ij} = \frac{1}{2}\left(\frac{\partial \overline{u}_i}{\partial x_j} + \frac{\partial \overline{u}_j}{\partial x_i} \right) \tag{5}$$

where δ_{ij} stands for the Kronecker delta and the strain rate tensor in the resolved field, $\overline{S}_{ij}$. ν_t is a function of $\overline{S}_{ij}$ and the subgrid length l.

$$\nu_t = l^2 \left| \overline{S}_{ij} \right| \tag{6}$$

$$l = C_s \overline{\Delta} \tag{7}$$

$$\left| \overline{S}_{ij} \right| = \sqrt{2 \overline{S}_{ij} \overline{S}_{ij}} \tag{8}$$

$\overline{\Delta}$ is the grid filter width, estimated as the cube root of the cell volume, and C_s is the Smagorinsky constant, here set to 0.2. The studies of Breuer [43 and 44] and Tremblay et al. [9] showed that the standard Smagorinsky model performs well in comparison to the more sophisticated subgrid scale models for similar type of flow. It was successfully used for the case of the single cylinder in the vicinity of the plane wall [26], for tandem cylinders in an infinite fluid [22] as well as for tandem cylinders close to the wall [8].

All the simulations are performed using the open source code OpenFOAM. The PISO algorithm (Pressure Implicit with Splitting of Operators) is used to solve the Navier-Stokes equations, described in [45]. For the time integration, implicit Crank-Nicolson method of second order is used. The spatial scheme for the convective and the gradient terms is Gauss linear, while Gauss linear with explicit non-orthogonal correction is used for the diffusive terms. All of the above schemes are of second order accuracy.

The code has been validated through the benchmark case of the flow around a single circular

cylinder in an infinite fluid and a uniform incident current at Re = 3.9 x 10^3 and Re = 1.31 x 10^4 (the same as in the present study). The details of the validation study were presented in Abrahamsen Prsic et al. [7]. The capabilities of the LES model (in OpenFOAM) were examined through the hydrodynamic coefficients, the time-averaged pressure distribution and the analysis of the flow field in the cylinder wake. The results in [7] compared well with previously published experimental and numerical results. Having in mind the similarity of the flow around a single cylinder with the geometry chosen in this study (from the perspective of turbulence modelling), the LES model implemented in the OpenFOAM code is chosen for the present study.

2.2. Computational set-up

The LES simulations are performed on the 3D rectangular computational domain extending (in x-direction) from 10D in front of the upstream cylinder centre to 30D behind the downstream one. The crossflow height of the domain is 10.5D+G, extending (in y-direction) from the rigid wall at 0.6D and 1D gap below the lowest part of the cylinders to 10D above the centre of the cylinders, see Figure 1. The spanwise length (z direction) is set to 4D. The domain dimensions are chosen in agreement with the previous research of the flow around a single cylinder in the vicinity of a plane wall and tandem cylinders in an infinite fluid, as well as in the vicinity of a wall, at Re = 1.31 x 10^4 [8, 26]. The domain dimensions are comparable to several previously published studies for tandem cylinders immersed in an unlimited flow, where it was shown that chosen distances are sufficiently large to eliminate the far-field effects of the boundaries. The details of the domain size choice are presented in [7, 26].

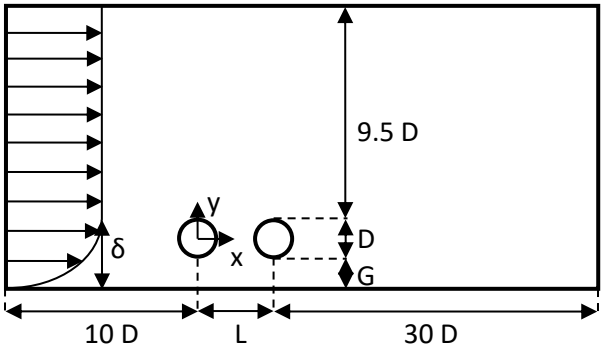

Figure 1. Computational domain definition sketch for the tandem cylinders in the vicinity of a plane wall. Inflow profile with the logarithmic boundary layer, δ/D = 0.48. In the present study, L/D = 2 and 5, G/D = 0.6 and 1. (Sketch is not in scale)

A body-fitted, structured O-mesh is divided into several zones (see Figure 2a), in order to maintain the control over the element size in the vicinity of the cylinders and at the bottom wall. The shape of the zones and the distribution of the elements through the domain are kept consistent for all cases. Special attention is paid to the transition between the zones in the vicinity of the cylinders, in order to obtain the smoothness of the mesh (Figure 2b). In all simulations, the size of the elements near the cylinders and the wall surface is chosen such that the maximum dimensionless wall surface distance η^+ is kept around 1. $\eta^+ = u_* \eta' / \nu$, where u_* denotes the friction velocity at the wall, and η' is the normal distance from the wall. The three-dimensional mesh is created by equidistantly aligning the two-dimensional meshes along the spanwise (z) axis. Simulations with several mesh refinements are performed for these combinations of key parameters: G/D = 0.6 and L/D = 2; G/D = 1 and L/D = 5, leading to the fully converged cases with up to 27 million elements, see Table 1. The detailed analysis of the convergence studies is given in the following section.

a)

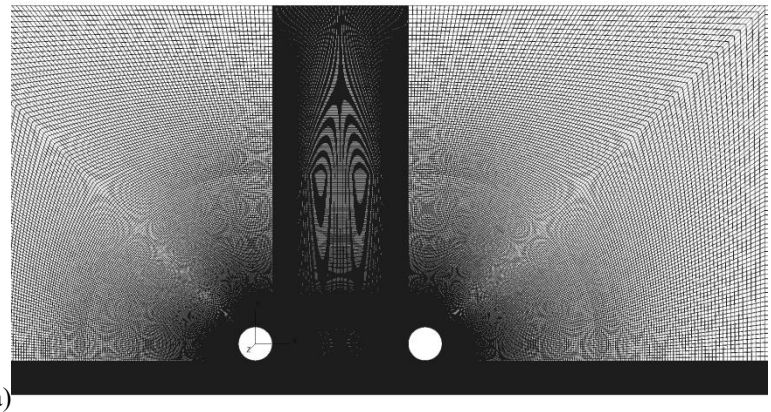

b)

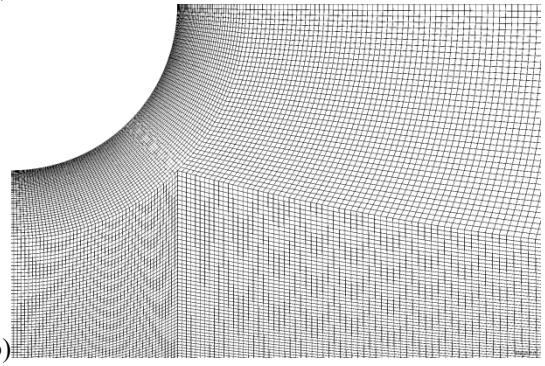

c)

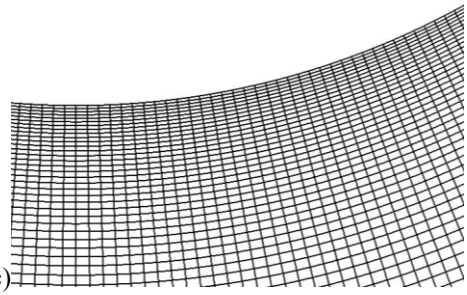

Figure 2. a) An overview over the mesh, cross-section of the domain in (x, y) plane.
b) Details of the mesh – the zones in the vicinity of cylinder 1. L/D = 5, G/D = 1.
c) Elements near the surface of the cylinders. L/D = 5, G/D = 1.

The boundary conditions are kept the same through the entire study. The inflow is specified by imposing the zero-gradient boundary condition for the pressure and the logarithmic velocity profile with a boundary layer thickness δ/D = 0.48 at the inlet. The vertically dependent inflow velocity profile is defined as

$$u(y) = \min\left\{\frac{u_*}{\kappa} ln\left(\frac{y}{z_w}\right), U_c\right\} \quad (9)$$

$$u_* = \frac{\kappa U_c}{\ln(\frac{\delta}{z_w})} \quad (10)$$

Here $\kappa = 0.41$ is the von Karman constant and $z_w = 1 \times 10^{-6}$m is the seabed roughness. A distance of 10D between the inflow and the upstream cylinder is chosen to ensure that the cylinder is exposed to the fully developed boundary layer logarithmic profile with the desired δ/D. The details can be referred to [26].

At the outlet, the pressure and the normal gradient of the velocity are set to zero. The top plane is defined as a symmetry boundary condition. The vertical side boundaries, perpendicular to the cylinders' axis, have the periodic boundary condition imposed, while the no-slip condition is applied on the surface of the cylinders and the bottom wall.

Table 1: Numerical set-up for the case of tandem cylinders close to the plane wall with L/D = 2 and 5, G/D = 0.6 and 1. Convergence studies.

Case name	Key parameter	gap G/D	spacing L/D	Total number of elements (million)	Dimensionless time-step Δt
G06 L2 m1	Mesh	0.6	2	12	0.00013
G06 L2 m2	Mesh	0.6	2	16	0.00013
G06 L2 m3	Mesh	0.6	2	20	0.00013
G06 L2	Mesh/time-step	0.6	2	24	0.00013
G06 L2 m5	Mesh	0.6	2	29	0.00013
G1 L5 m1	Mesh	1	5	12	0.00013
G1 L5 m2	Mesh/time-step	1	5	16.5	0.00013
G1 L5 m3	Mesh	1	5	21	0.00013
G1 L5	Mesh	1	5	25	0.00013
G1 L5 m5	Mesh	1	5	32.7	0.00013
G1 L5 t3	Time-step	1	5	25	0.00033
G1 L5 t2	Time-step	1	5	25	0.00065
G1 L5 t1	Time-step	1	5	25	0.00098

3. Grid and time-step refinement studies

The grid and the time-step refinement studies are performed for the flow around the tandem circular cylinders in the vicinity of a plane wall at Re = 1.31 x 10^4. The cylinders are placed at G/D = 0.6 and 1 with the longitudinal spacing ratio L/D = 2 and 5. These two G/D and L/D combinations are chosen to represent the diversity of the flow, including the narrow and the wide gap regimes, as well as the reattachment and the co-shedding regimes.

The influences of the mesh refinement and the choice of the time-step are analysed through the values of the time- and space-averaged drag coefficients ($\overline{C_{d1}}$ and $\overline{C_{d2}}$ represent the mean drag coefficients for the upstream and the downstream cylinder, respectively) and the root-mean-square (rms) of the space averaged lift coefficients (C_{lrms1}, C_{lrms2} represent the upstream and the downstream cylinder, respectively, where $C_{lrms} = \overline{(C_l^2)}^{1/2}$). The comparison through normalized time- and space-averaged velocity profiles in the cylinders' wake is presented at the end of this section. The aforementioned drag ($C_{dl,2}$) and lift ($C_{l1,2}$) coefficients for the cylinders are defined as: $C_{dl,2} = F_{dl,2}/(0.5\rho U_\infty^2 A)$ where $F_{dl,2}$ is the drag force exerted on the upstream/downstream cylinder and obtained by integrating the pressure over the cylinder surface. A is the projected frontal area of each cylinder; $C_{l1,2} = F_{l1,2}/(0.5\rho U_\infty^2 A)$, where $F_{l1,2}$ is the integrated lift force. The time averaging is done for the fully developed flow.

In order to perform the grid refinement study, five different meshes are created for each of the aforementioned G/D and L/D combinations. The meshes are proportionally refined in all directions and all zones. General characteristics of the meshes, such as the distribution of the zones, the elongation and the skewness of the elements are kept the same for all five simulations. The size of the elements at the cylinder surface and the plane wall surface is also kept nearly constant for all simulations, in order to keep $\eta^+ < 1$. Details about the cases are given in Table 1.

In the case with G/D = 1 and L/D = 5, the results presented in Figure 3a and 3b, and Table 2, suggest that convergence is approached in the G1 L5 case. Between the coarsest and the finest mesh, variations of all coefficients are within 10%. Variations of both the drag and the lift coefficients are small and do not show a steady trend. This behaviour suggests that the convergence is nearly achieved already for the coarser mesh cases. The overall mesh refinement leads to a slight decrease in the drag and the lift coefficients of both cylinders, with changes between 1% and 5%. It is therefore concluded that the convergence is obtained and the mesh with 25 million elements (case G1 L5, see Table 1) provides a sufficient grid resolution.

The values of the drag and the lift coefficients with mesh refinement in the case with G/D = 0.6 and L/D = 2 are presented in Figure 3c and 3d. Here, the mean flow coefficients behave similarly to the previously presented grid convergence study for G/D = 1 and L/D = 5. The overall changes in $\overline{C_{d1}}$, $\overline{C_{d2}}$ and C_{lrms2} are within 10%. C_{lrms1} varies with 30%. Here, it is important to have in mind the very low values for C_{lrms2} in the cases of small L/D = 2 (see Table 2) and consequently very small absolute change in C_{lrms2} through the mesh refinement. These results point to the conclusion that the mesh used in the case G06 L2 is sufficiently fine.

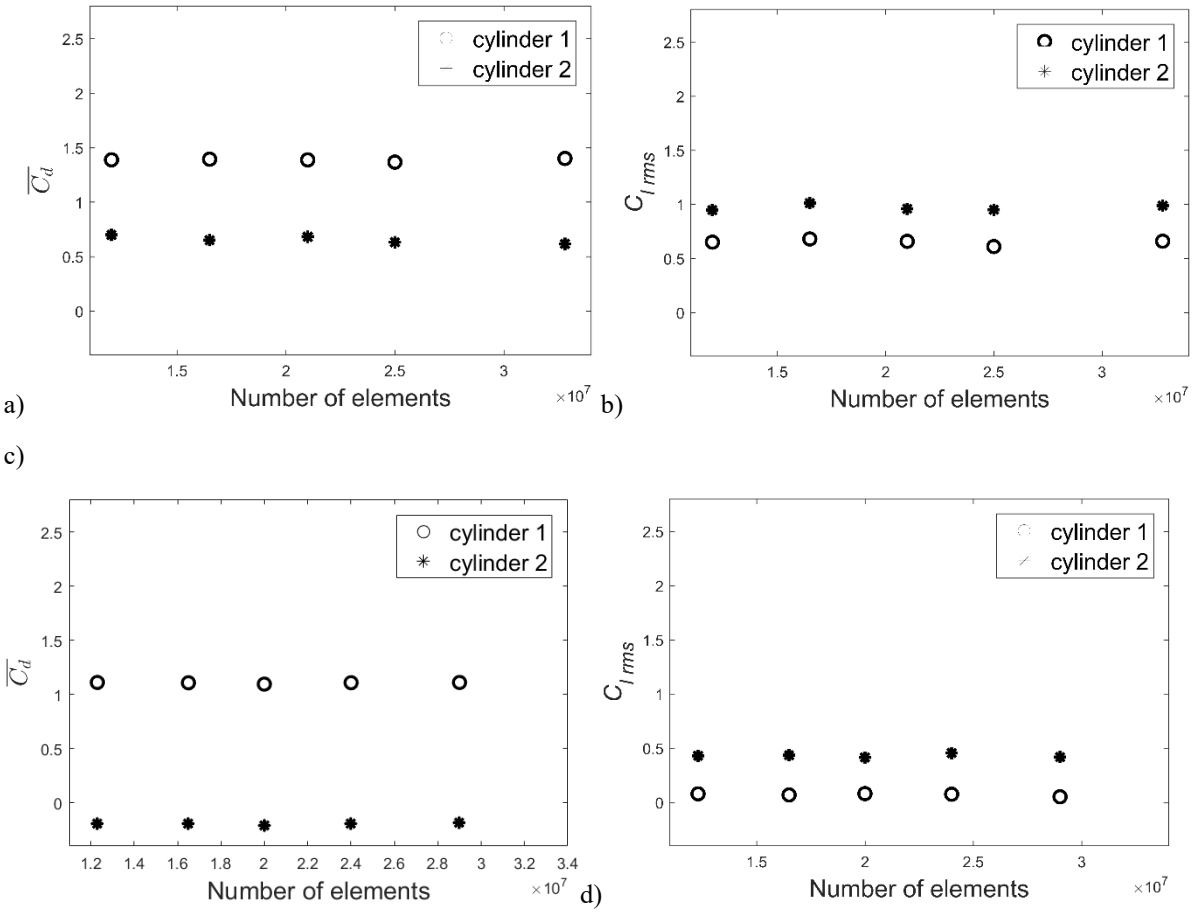

Figure 3. The grid convergence study.

a) $\overline{C_{d1}}$ and $\overline{C_{d2}}$; G/D = 1, L/D = 5.

b) $C_{l\,rms1}$ and $C_{l\,rms2}$, G/D = 1, L/D = 5.

c) $\overline{C_{d1}}$ and $\overline{C_{d2}}$; G/D = 0.6, L/D = 2.

d) $C_{l\,rms1}$ and $C_{l\,rms2}$, G/D = 0.6, L/D = 2.

Similar analysis is made for the time-step convergence study. Dimensionless time-steps of Δt = 0.00098, 0.00065, 0.00033 and 0.00013 are used in the simulations with G/D = 1 and L/D = 5 (see Table 1). In all simulations, Courant number is kept well below one. The mean Courant number does not exceed 0.02 in any case, while the maximum in-cell Courant number obtains the following values, approximately 0.38, 0.23, 0.11 and 0.05 respectively. Values of the mean drag and the rms lift coefficients are presented in Figure 4, revealing a mild trend and small variations. Table 2 shows that the variations of $\overline{C_{d1}}$ are within 5%, $\overline{C_{d2}}$ decreases 8% as the time-step decreases. C_{lrms1} varies with 17% and C_{lrms2} with 9%. It should be noticed that the changes of the integrated forces on the cylinders are not uniformly increasing or decreasing, but are in all cases small. This is attributed to the fact that the convergence is already approached at the larger time-steps, while further refinement leads to small improvements in the mean forces. This conclusion is also confirmed by Abrahamsen Prsic et al. [8, 26], who conducted a time-step refinement study for a single and tandem cylinders in the vicinity of a plane wall, with the same Re and G/D as here, and reported it to be a robust factor. The time-step of 0.00013 is therefore considered to be sufficient for further analysis.

Table 2: Mean flow parameters for the tandem cylinders close to the plane wall at L/D = 2 and 5, G/D = 0.6 and 1. Convergence studies.

Case name	Key parameter	$\overline{C_{d1}}$	$\overline{C_{d2}}$	C_{lrms1}	C_{lrms2}
G06 L2 m1	Mesh	1.110	-0.191	0.079	0.431
G06 L2 m2	Mesh	1.107	-0.191	0.069	0.435
G06 L2 m3	Mesh	1.095	-0.210	0.081	0.415
G06 L2	Mesh/time-step	1.107	-0.193	0.076	0.455
G06 L2 m5	Mesh	1.110	-0.188	0.052	0.419
G1 L5 m1	Mesh	1.388	0.699	0.660	0.948
G1 L5 m2	Mesh	1.394	0.651	0.681	1.011
G1 L5 m3	Mesh	1.388	0.682	0.658	0.959
G1 L5	Mesh/time-step	1.387	0.631	0.611	0.951
G1 L5 m5	Mesh	1.398	0.616	0.660	0.988
G1 L5 t3	Time-step	1.313	0.653	0.540	0.926
G1 L5 t2	Time-step	1.364	0.709	0.602	0.952
G1 L5 t1	Time-step	1.323	0.662	0.530	0.896

In order to further investigate the influence of the numerical grid, the wake velocity profiles are examined and the streamwise velocity component is presented in Figure 5b and 5c, for the two investigated configurations. For all cases in this study, the velocity fields are averaged in time for the fully developed flow. The streamwise velocity component is further averaged in spanwise direction over 15 equidistant cross-sections distributed in the (x, y) plane. This time- and spanwise-averaged streamwise velocity is presented over the cross-sections in the wake of both cylinders, schematically indicated in Figure 5a.

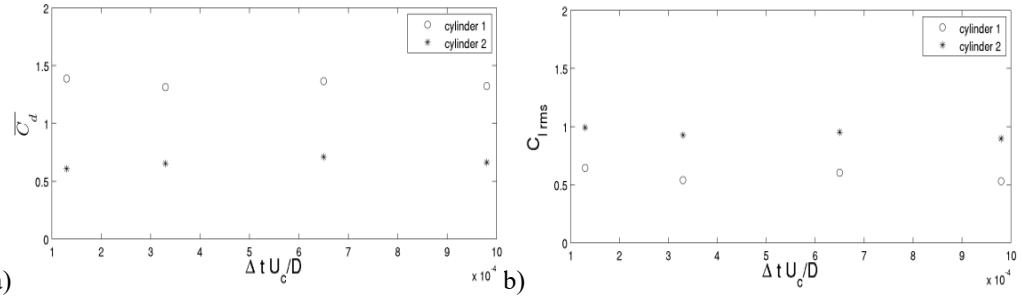

a) b)

Figure 4. The time-step convergence study. L/D = 5 and G/D = 1. Cases G1 L5 t1 (Δt = 0.00098), G1 L5 t2 (Δt = 0.00065), G1 L5 t3 (Δt = 0.00033) and G1 L5 (Δt = 0.00013).

a) $\overline{C_{d1}}$ and $\overline{C_{d2}}$;

b) $C_{l\,rms1}$ and $C_{l\,rms2}$.

The strongest influence of the mesh refinement manifests itself in the gap between the cylinders at L/D = 5 and G/D = 1. A large gap and spacing ratio allow the vortex shedding from the upstream cylinder to fully develop; resulting in a complex flow with large vortices interweaved with smaller vortical structures. Unlike the flow around a single cylinder, where the wake flow freely dissipates in the far wake, in the case of tandem cylinders, it meets the other cylinder and its boundary layer flow. A fine mesh, capturing the evolution of the vortical structures between the cylinders is thus important for this study. The mesh refinement leads to a somewhat shorter recirculation length of the upstream cylinder, and lower streamwise velocity in the spacing, as seen in Figure 5b. The behaviour of the downstream cylinder wake shows less sensitivity to the mesh refinement, leading to slightly slower velocity recovery for the fine meshes (Figure 5b). The wake velocity profiles for the two finest meshes are in very good agreement, pointing that the G1 L5 case has sufficient grid resolution.

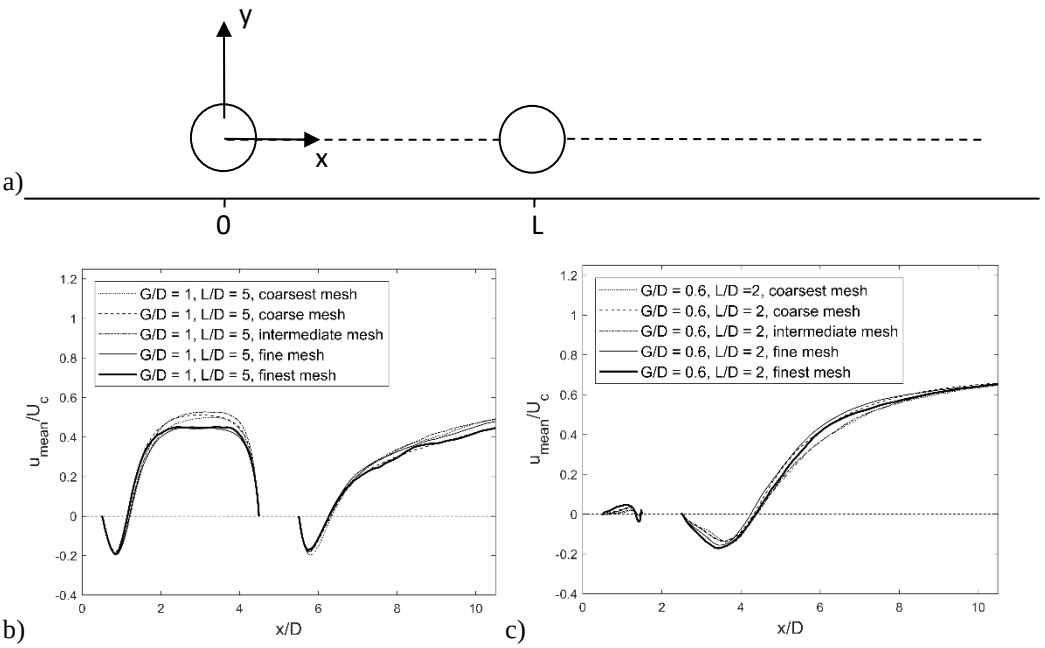

a)

b) c)

Figure 5. a) Definition sketch of the positions for the mean streamwise velocity sampling.

b) Normalized time- and spanwise-averaged streamwise velocity (u_{mean}/U_c) profiles for G/D = 1 and L/D = 5, grid refinement study.

c) Normalized time- and spanwise-averaged streamwise velocity (u_{mean}/U_c) profiles for G/D = 0.6, L/D = 2, grid refinement study.

The smaller G/D = 0.6 and L/D = 2 reduce the velocities in the wake of the upstream cylinder. The velocities between the cylinders are thus smaller, and a good grid resolution is essential for capturing the interaction of the boundary layers and the shear flow. Figure 5c shows that the finer meshes capture slightly higher velocities in the spacing and the near wake of the downstream cylinder. The differences are, however, small, leading to the conclusion that the mesh used in G06 L2 case (see Table 1) has sufficient resolution.

4. Results

Influences of two parameters, the distance between the tandem cylinders and the vicinity of the plane wall, are examined in this chapter. Four combinations with L/D = 2 and 5 as well as G/D = 0.6 and 1 are chosen. The setup parameters and details of the numerical cases are presented in Table 3. Since there is very limited data published about the tandem cylinders in the vicinity of a wall, the parameters in this study are chosen such that the present results can be compared to the more commonly examined cases – a single cylinder close to a plane wall and tandem cylinders in uniform flow.

Through the comparisons, one should keep in mind the influence of Re. Re = 1.31 x 10^4, used in this study, belongs to the subcritical flow regime ($300 < Re < 3 \times 10^5$), more precisely in TrSL2 (transition-in-shear-layers sub-regime, $2000 < Re < 40000$, see [2]).The resulting flow has laminar separation at the upstream cylinder and transition to turbulence in the near cylinder wake, with a 3D vortex street. This is also the regime where the fluid forces exerted on a single cylinder in a uniform flow are comparatively insensitive to the changes in Re [15]. The present results are therefore compared to the previously published studies of the flow in the subcritical regime, at comparable Re.

In the case of tandem cylinders at L/D = 5, the downstream cylinder is sufficiently far away that the von Karman vortex shedding develops both on the upstream and the downstream cylinder [18]. The wake of each cylinder close to a wall is thus comparable to the flow around a single cylinder in the vicinity of the wall. On the other hand, a single cylinder in the wide gap regime, especially in the case of G/D = 1, experiences only marginal wake alterations due to the presence of the wall. Therefore the present case of two cylinders with large G/D can be compared to the case of tandem cylinders in an infinite fluid.

In Section 4.1, the present results are placed within the classifications of the aforementioned cases of a single cylinder close to a wall and the tandem cylinders in infinite fluid. The data is analysed through the mean values and the time development of the hydrodynamic coefficients as well as through the behaviour of the flow fields behind the cylinders. Sections 4.2 and 4.3 focus on the specific effects of the spacing ratio and the gap ratio. The main flow phenomena are discussed through the time-averaged values of flow fields, while the instantaneous values offer an insight into the details of the wake flow and the dynamic nature of the wakes behind each cylinder.

Table 3: Numerical set-up for the case of tandem cylinders close to the plane wall at L/D = 2 and 5, G/D = 0.6 and 1.

Case name	G/D	L/D	Total number of elements (million)
G06 L2	0.6	2	24
G06 L5	0.6	5	24.5
G1 L2	1	2	21
G1 L5	1	5	25

4.1. Classification of the flow

Depending on the distance between the two cylinders, as well as the distance from the plane wall, different types of wake flow are obtained. According to previously published research, the critical gap to diameter ratio divides the flow around a single cylinder between the narrow and the wide gap regime. The experimental research of Bearman and Zdravkovich [46] placed the critical G/D at 0.3 – 0.4. Re-examination of the wall effects by Lei et al. [47] identified it between 0.2 and 0.3. While the narrow gap regime suppresses the vortex shedding, the term wide gap regime covers a broad variety of vortex shedding types. According to [27], regular vortex shedding occurs for G/D > 0.5. However, the influence of the wall is noticeable at G/D = 0.6, manifested through less prominent vortex shedding and an elongated wake deflected away from the wall [26]. At G/D > 1, the separation of the wall boundary layer vanishes both upstream and downstream of the cylinders and the flow is comparable to that around a single cylinder in the infinite fluid ([1] and [13]).

The flow around tandem circular cylinders in unlimited fluid is coarsely classified according to the critical spacing ratio. At spacing ratios smaller than the critical, the vortex shedding from the upstream cylinder is suppressed, while larger spacing allows development of a vortex street [13]. An example of more detailed classification is presented in [16]. Three main regimes are recognized. Tandem cylinders with L/D between 1 and 2 yield the extended body regime, where the tandem cylinders behave as a single elongated body. At L/D between 2 and 5, the upstream cylinder shear layers reattach on the downstream cylinder, leading to the reattachment regime. At even larger L/D, the flow around the upstream cylinder is not affected by the downstream one, and the vortices shed from it impinge periodically on the downstream cylinder, resulting in the impinging regime.

4.1.1. Drag and lift coefficients

At L/D = 5, large distance between the tandem cylinders allows the development of vortex shedding from both cylinders [8]. The mean flow parameters ($\overline{C_{d1}}$,C_{lrms1}) of the upstream cylinder are therefore compared to the values for the single cylinder near a plane wall. According to [13], for a single cylinder in the vicinity of the plane wall, decrease in G/D leads to a decrease in the values of the mean flow parameters. [1] found that this influence subsides at G/D around 1. Measurements by Lei et al. [47] and the numerical results by Abrahamsen Prsic et al. [8] for G/D = 1 confirmed this, finding only a small decrease in $\overline{C_d}$ and C_{lrms} values for a single cylinder close to a wall. The present $\overline{C_{d1,2}}$ and $C_{lrms1,2}$ values (see Table 4, case G1 L5) are in good agreement with the values presented by Alam et al. [15] for L/D = 5 at Re = 6.5 x 10^4 and LES for the case of a single cylinder at G/D = 1 by Abrahamsen Prsic et al. [26].

Table 4: Mean flow parameters for the tandem cylinders close to the plane wall. Present study: L/D = 2 and 5, G/D = 0.6 and 1, and previously published results.

Case name/author	Re	L/D	G/D	$\overline{C_{d1}}$	$\overline{C_{d2}}$	C_{lrms1}	C_{lrms2}
G06 L2	1.31×10^4	2	0.6	1.11	-0.19	0.08	0.46
G06 L5	1.31×10^4	5	0.6	1.07	0.53	0.12	0.40
G1 L2	1.31×10^4	2	1	1.10	-0.26	0.02	0.34
G1 L5	1.31×10^4	5	1	1.39	0.63	0.61	0.95
Igarashi [49]	3.55×10^4	2.09 5	∞	1.03 1.31	-0.32 0.47		
Ljungkrona et al. [48]	2×10^4	2 5	∞	0.93 1.20	-0.39 0.50		
Alam et al. [15]	6.5×10^4	2 5	∞	1.05 1.22	-0.24 0.29	0.03 0.44	0.55 0.71
Kitagawa and Ohta [22]	2.2×10^4	2 5	∞	0.88 1.17	0.02 0.50	0.13 0.20	0.58 1.00
Abrahamsen Prsic et al. [26]	1.31×10^4	One cyl.	0.6 1	1.06 1.44		0.12 0.71	
Wang et al. [34]	6.3×10^3	2 5 2 5	0.6 0.6 1.4 1.4		0.06 0.48 -0.04 0.6		0.08 0.17 0.18 0.50

$\overline{C_{d1}}$ is in very good agreement with [26], and C_{lrms1} obtains exactly the same value as for a single cylinder. It is thus concluded that, at L/D = 5, the mean hydrodynamic forces exerted on the upstream cylinder are not affected by the presence of the downstream cylinder.

The upstream cylinder in a tandem arrangement close to the plane wall is exposed to an incoming flow with a smoothly developed boundary layer profile, similar to what a single cylinder would experience. On the other hand, the downstream cylinder is immersed in a highly turbulent flow and exposed to large vortices periodically shed from both sides of the upstream cylinder. This results in a significantly lower value of the mean drag coefficient at G/D = 0.6 and 1 (L/D = 5 in both cases). This is also captured in the LES results for the tandem cylinders in an unlimited fluid presented by Kitagawa and Ohta [22] and Sainte-Rose et al. [24], as well as the measurements of Ljungkrona et al. [48]. The experimental results for the tandem cylinders in the vicinity of the plane wall by Wang et al. [34] show a similar decrease in $\overline{C_{d2}}$ compared to a single cylinder, as well as the decreasing trend of $\overline{C_{d2}}$ with narrowing of the gap. At large L/D = 5, the present results are in good agreement with the experiments, within 10%.

The smaller L/D = 2 implies a stronger interaction between the cylinders. Experimental results for the flow around tandem cylinders in an infinite fluid by Zdravkovich and Pridden [12] at $Re = 3.1 \times 10^4$, Igarashi [49] at $Re = 3.55 \times 10^4$ as well as Ljungkrona et al. [48] using $Re = 2 \times 10^4$, show negative $\overline{C_{d2}}$ for L/D < 3. Their results are in good agreement with the present values for the case at G/D = 1. $\overline{C_{d2}}$ measured by Wang et al. [34] for the tandem cylinders with $Re = 6.3 \times 10^3$ obtained positive value for G/D = 0.6 and negative value for G/D = 1.4. However, the measured $\overline{C_{d2}}$ has small absolute values and the reduction compared to $\overline{C_{d1}}$ is significant, with the decreasing trend for the decreasing gap, as in this study.

The time histories of the drag and the lift coefficients on both cylinders are presented in Figure 6. In the case with L/D = 5 and G/D = 1, strong, periodic oscillations can be noticed for both C_{d1} and C_{d2} (Figure 6a), as well as C_{l1} and C_{l2} (Figure 6c). The amplitudes of both coefficients are more prominent for the downstream cylinder and, while the time history of C_{d2} shows some irregularities, C_{l2} oscillates smoothly. This behaviour is also reported by Wang et al. [34] as well as by Kitagawa and Ohta [22]. It confirms that, despite the presence of the wall, the case with G/D = 1 and L/D = 5 clearly behaves as tandem cylinders in co-shedding regime. At L/D = 5, narrowing the gap to G/D = 0.6 results in reduction of the C_{d1} oscillations (Figure 6b) and a significant reduction of the C_{l1} amplitude (Figure 6d). This behaviour resembles the case of a single cylinder at G/D = 0.6 ([47] and [26]). C_{d2} and C_{l2} also oscillate with reduced amplitudes (in agreement with [34]), but their periodicity indicates regular vortex shedding from the downstream cylinder.

For both gaps (G/D = 0.6 and 1), time series of the flow parameters show an inherent difference of the cases with L/D = 2 and 5. The smaller spacing ratio hinders periodic C_{d1} and C_{l1} oscillations, while only small amplitudes without regular periodicity are observed for the downstream cylinder. In case of the isolated tandem cylinders at L/D = 2 [22], the behaviour of the flow coefficients on the leading cylinder is similar as in the present study. The flow around the downstream cylinder in the unlimited fluid, on the other hand, shows clearer periodicity and larger oscillations in C_{l2} than in the present study.

Due to only mild effect of the wall at relatively large distance from the plane wall, G/D = 1, the flow is comparable with the results for the tandem cylinders in an infinite fluid and a uniform current. In [22], they used LES to simulate the flow around tandem cylinders in unlimited fluid with L/D between 2 and 5, at $Re = 2.2 \times 10^4$. Kitagawa and Ohta [22] and Sainte-Rose et al. [24] report that the time histories showed irregularities in the periodic oscillations of C_{d1} and C_{d2}, similar to the present study and contrary to the uniformly oscillating drag coefficient for one isolated cylinder. However, in both studies of the flow around tandem cylinders in an unlimited fluid, a single dominant amplitude can be identified. In the present study, however, C_{d2} for the case with G/D = 1 and L/D = 5 shows alternating strong and weak oscillations (Figure 6a). The co-shedding regime, also called the impinging regime [11], indicates a strong influence of the vortices shed from the upstream cylinder colliding with the downstream one. Since the vortices shed from a single cylinder at G/D = 1 become deformed by the wall as they move farther downstream in the cylinder wake [26], the alternating amplitudes of C_{d1} and C_{d2} (Figure 6a and 6b) might be attributed to the asymmetric impingement. Details of the flow between the cylinders are further discussed in Section 4.2.

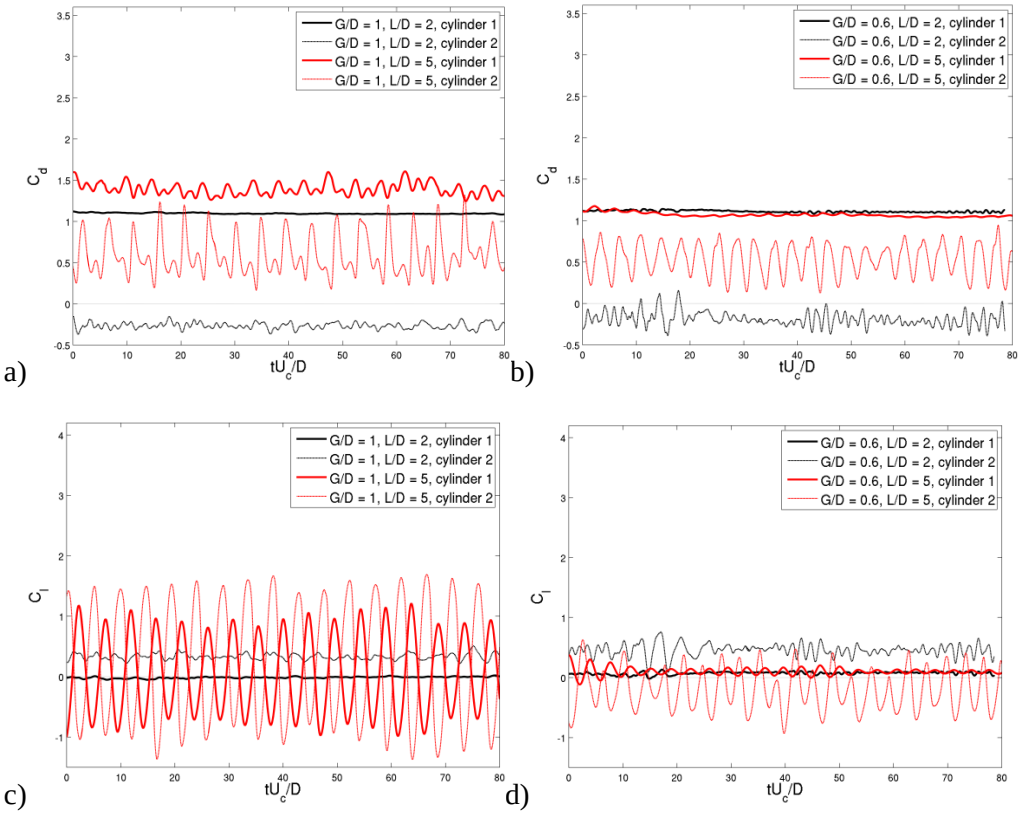

Figure 6. Time histories of the drag and the lift coefficients. L/D = 2 - black line, denoted as L2, L/D = 5 - red line, denoted as L5. Upstream cylinder (cylinder 1) - thick line, downstream cylinder (cylinder 2) – thin line.
a) and c) $C_{d1,2}$ and $C_{l1,2}$ for G/D = 1.
b) and d) $C_{d1,2}$ and $C_{l1,2}$ for G/D = 0.6.

The time series of the lift coefficients for the cases with L/D = 5 are periodic, with slowly varying amplitude. Comparing C_{lrms1} to C_{lrms2} in the cases with G/D = 0.6 and 1 (Table 4), a significantly larger amplitude is observed for the downstream cylinder. In cases with both G/D, despite the difference in the amplitudes, both cylinders undergo vortex shedding at the same frequency. This is in agreement with Alam and Zhou [50], who concluded that, in the case of tandem cylinders in the infinite fluid, the vortex shedding from the downstream cylinder is triggered by the arrival of the vortices from the upstream one. Vortex shedding at the same frequency from both cylinders is also observed in the numerical results [22] and [23]. While the present results give larger C_{l2} amplitudes than measured by Wang et al. [34] for the tandem cylinders at G/D = 0.6 and 1.4, the overall behaviour is in good agreement. Similar to the present study, they report periodic oscillations of C_{l2} for G/D = 1.4, with small variations in amplitude, and significantly lower C_{lrms2} for G/D = 0.6, with larger variations and less periodicity.

4.1.2. Details of the wake flow

The periodicity in the wake of the downstream cylinder is reflected in the energy spectra, presented in Figure 7 for the cases with G/D = 1 and L/D = 2 and 5. The spectra are presented for the energy sampled by a numerical probe at each time-step in single point behind the downstream cylinder (x/D = 2.5 for G/D = 1 and L/D = 2; x/D = 5.5 for G/D = 1 and L/D = 5, y/D = 0.25, z/D = 2 in both

cases). The frequencies (f) are normalized (f_{St}) to correspond Strouhal number (St), $f_{St} = fD/U_c$. Here, the thin line denotes the Kolmogorov -5/3 spectrum, see Mathieu and Scott [51].

The energy spectrum of the downstream cylinder wake at L/D = 5 shows the energy maximum at St = 0.2, indicating the presence of periodic vortex shedding. This value is in good agreement with the measurements of Wang et al. [34], reporting St = 0.19. Another strong peak is visible approximately at double St frequency for the case with G/D = 1 and L/D = 5 (Figure 7). The presence of the second harmonic is in agreement with the time-series of $C_{d1,2}$ indicating the alternating high and low amplitude (Fig. 6a). On the other hand, the absence of any prominent maximum in the Strouhal number for L/D = 2 confirms the previous discussion about the suppression of the vortex shedding from the downstream cylinder in the narrow spaced tandem.

The mean streamwise velocity contours (Figure 8) offer an insight in the general characteristics of the wakes of tandem cylinders in the vicinity of the wall. The previous conclusion that the upstream cylinder is not affected by the downstream one for the L/D = 5 cases is here confirmed. By comparing with the single cylinder at G/D = 1 (Figure 8a), the wake of the upstream cylinder in the cases with G/D = 1 and L/D = 5 (Figure 8c) shows the same type of relatively short and symmetric wake with only mild acceleration of the flow underneath the cylinder. The case with G/D = 0.6 and L/D = 5 (Figure 8d) shows the same main characteristics as the flow around a single cylinder at G/D = 0.6 (Figure 8b), i.e. the elongated primary separation bubble deflected form the wall and significant alterations in the bottom wall boundary profile far behind in the cylinder wake.

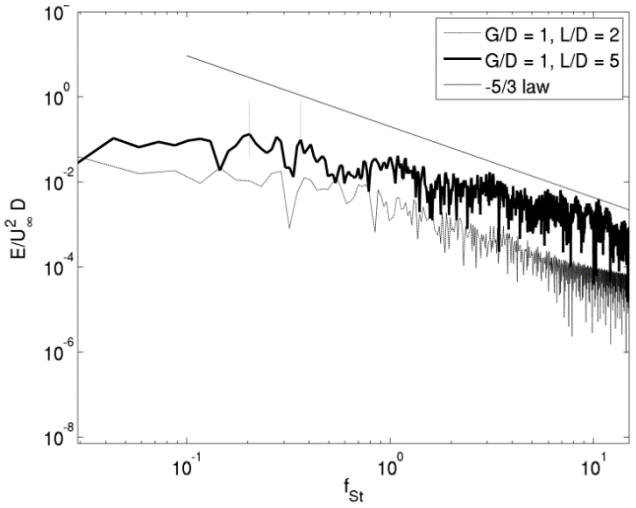

Figure 7. Energy spectra in the wake of the downstream cylinder for G/D = 1 and L/D = 2 (thin line) and G/D = 1 and L/D = 5 (thick line). Dotted lines denote the energy maxima corrsponding to the first and the second harmonic of the vortex shedding frequency. $f_{St} = fD/U_c$.

The wake of the downstream cylinder, on the other hand, shows altered behaviour. Similar to the conclusions in [16], the wake of the downstream cylinder in the case with G/D = 1 and L/D = 5 is somewhat broader and more dispersed (also reported in [23]), as well as less symmetric. This can be attributed to the deformation of the vortices shed from the lower half of the upstream cylinder as they encounter the bottom wall. Despite the obvious differences in the upstream cylinder wakes for the cases G1 L5 (Figure 8c) and G06 L5 (Figure 8d), the near wakes of the downstream cylinders show more similarities. This significant shortening of the wake, compared to the upstream cylinder for the G06 L5 case, and the absence of the secondary recirculation at the bottom wall boundary, was also captured experimentally by Wang et al. [34]. It is thus concluded that the inflow on the downstream cylinder,

shaped by the strong vortices shed from the upstream cylinder, is the key factor in the development of the downstream cylinder wake. The vicinity of the bottom wall plays a secondary role, deforming the incoming vortices.

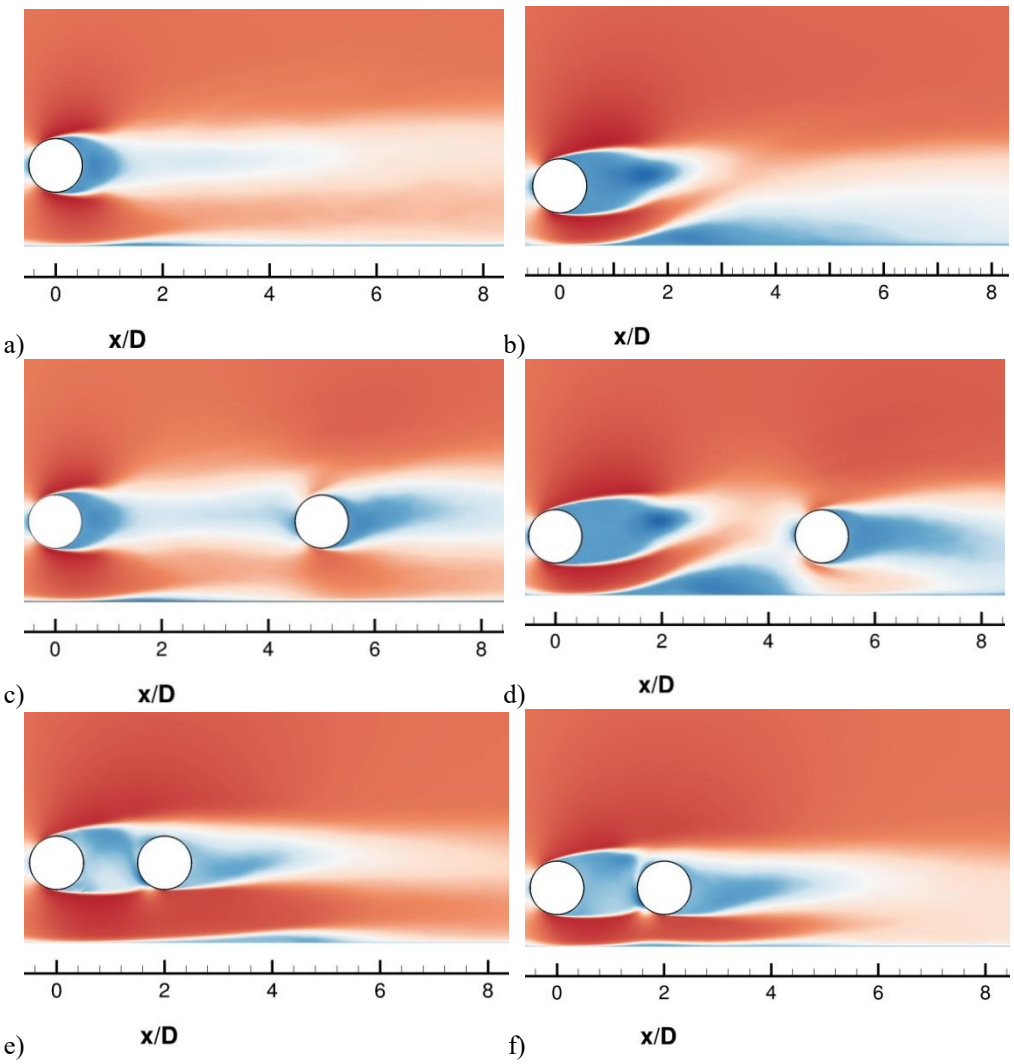

Figure 8. Time-averaged streamwise velocity contours, cross-section at the middle of the cylinder span. Red – positive vaølues, blue - negative.

a) Single cylinder in the vicinity of the wall, G/D = 1, case G1 1 presented in [26];
b) Single cylinder in the vicinity of the wall, G/D = 0.6, case G06 1 presented in [26];
c) Tandem cylinders at G/D = 1 and L/D = 5;
d) Tandem cylinders at G/D = 0.6 and L/D = 5;
e) Tandem cylinders at G/D = 1 and L/D = 2;
f) Tandem cylinders at G/D = 0.6 and L/D = 2 (c – f, present study).

The flow around the upstream cylinder at L/D = 2 is strongly influenced by the presence of the downstream one. At G/D = 1, the influence of the wall on a single cylinder's wake is almost negligible. Horizontally narrow placed tandem cylinders experience stronger wall interaction due to the "extended body" effect. The upstream cylinder wake in the case with G/D = 1 and L/D = 2 (Figure 8e) shows asymmetry, similar to the smaller gap case (G/D = 0.6 and L/D = 2, Figure 8f). For both G/D, the downstream cylinder yields an elongated wake, with a slight deflection form the wall. The same wake behaviour is captured in [34]. The absence of the regular vortex shedding, which is a dominant factor in the L/D = 5 cases, allows the effects of the wall to emerge.

A cylinder wake can also be investigated through the recirculation length (Lr), defined as the distance between the cylinder base and the point of zero streamwise mean velocity in the wake. At L/D = 2, the standard recirculation is not developed in the small spacing between the cylinders (Figure 9a). The discussion of Lr is thus obsolete. On the other hand, the near wake of the upstream cylinder at L/D = 5 obtains the shape recognizable from the case of one cylinder near the plane wall [26]. The mean streamwise velocity profiles behind the upstream cylinder for the cases with G/D = 0.6 and 1, L/D = 5 (Figure 9b) show an increase in Lr as the gap decreases. This trend is similar to the case of a single cylinder near the wall reported by Wang and Tan [29]. In the wake, between x/D = 2 and 4, the mean streamwise velocity in the G/D = 0.6 and L/D = 5 case obtains higher values than in the case with G/D = 1 and L/D = 5. This is attributed to the fact that the smaller gap causes a longer wake, also deflected from the wall. The smaller velocities in the recirculation area, are thus located farther from the wall, allowing the higher velocity flow created in the gap between the cylinder and the wall to permeate higher in the spacing between the cylinders. The elongation of the wake with the narrower gap is also present in the wakes of the downstream cylinders in cases with G/D = 0.6 and 1, L/D = 5.

At spacing L/D = 2, cases with G/D = 0.6 and 1 show comparable downstream cylinder wake profiles (Figure 9a). However, for both G/D, the downstream cylinders in the L/D = 2 cases obtain larger Lr than with large spacing ratio. The recovery of the velocity in the wake, 2 to 5D behind the downstream cylinder, is considerably slower for the L/D = 5 cases. This is attributed to the highly turbulent inflow from the upstream cylinder, contrary to the more restricted flow in the gap between the cylinders at L/D = 2.

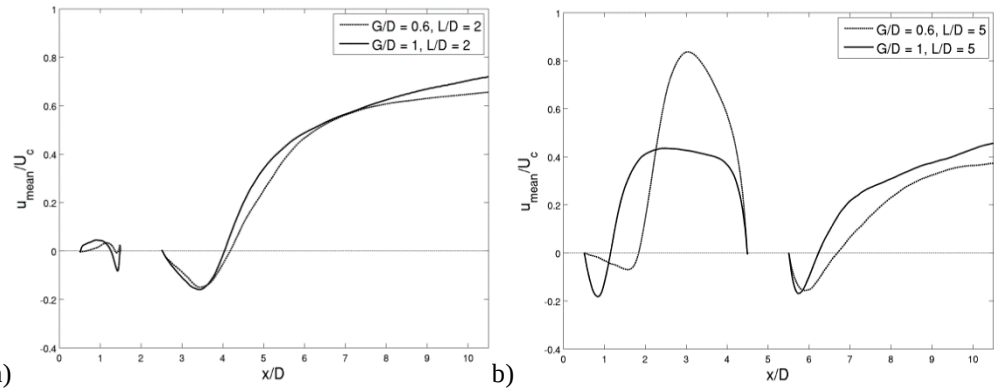

a) b)

Figure 9. Normalized time- and spanwise-averaged streamwise velocity (u_{mean}/U_c) profiles. y/D =0.
a) L/D = 2, G/D= 0.6 and 1;
b) L/D = 5, G/D= 0.6 and 1.

4.2. Influence of the spacing ratio

The more specific details of the flow are observed through the instantaneous values of velocity, vorticity and pressure fields in this section. The spanwise vorticity (ω_z) is presented through 4 snapshots over one vortex shedding period for the cases with G/D = 1 and L/D = 2 (Figure 10) as well as G/D = 1 and L/D = 5 (Fig. 11). By comparing Figures 10 and 11, the differences in the wake flow are clearly noticeable. While L/D = 2 causes inhibition of the vortex shedding from the upstream cylinder and the narrow wake behind the downstream one, broad von Karman vortex streets appear in the wakes of both cylinders at the large spacing ratio.

The cases are also compared to the flow around tandem cylinders in an infinite fluid. Indeed,

the same characteristics of the wake flow are captured in the smoke wind tunnel experiments by Igarashi [49] at Re = 1.3 x 10^4, as well as by Ljungkrona and Sunden [52] for Re = 1.2 x 10^4. Due to the nature of the measurements, these experimental results are not depicting the fine structures in the area between the cylinders and in the near wakes; neither could they be suitable for representing the complex flow in the gap between the cylinders and the wall. The present study is therefore utilized to complement the experimental conclusions.

Compared to the case of a single cylinder near the wall, for both spacing ratios, the vortices shed from the downstream cylinder are formed closer to the cylinder base. The same behaviour is observed for the tandem cylinders in an infinite fluid at L/D = 2 by Meneghini et al. [20] and for L/D = 5 by Zhou and Yiu [16]. Furthermore, the wake of the downstream cylinder changes due to the spacing ratio. Similar to the conclusions of Igarashi [49] and Lin et al. [14], the smaller spacing ratio L/D = 2 yields a narrower wake with elongated von Karman vortices, while L/D = 5 results in larger and weaker vortices. This broad and symmetric wake is observed in [16]. However, the presence of the wall in the G/D = 1 and L/D = 5 case distorts the vortices shed from the bottom half of the upstream cylinder, causing the asymmetric impingement on the downstream one. This behaviour manifests in the alternating amplitude of C_{d2} oscillations, discussed in Figure 6a.

For the tandem cylinders in the infinite fluid, the configurations with very small spacing ratios is called the extended body (or single bluff body) regime [18]. Here, the shear layers separated from the upstream cylinder wrap around the downstream one without reattachment. According to the classification in [16], the transition to the reattachment regime happens at L/D = 2, while [11] defines the single bluff body regime up to L/D = 1.2 – 1.8. From the behaviour of the vorticity presented in Figure 10, at L/D = 2 and G/D = 1, the present flow resembles the reattachment regime. In the case of the isolated tandem cylinders, the alternating reattachment on the downstream cylinder was reported by Ljungkrona and Sunden [52] and Kitagawa and Ohta [22]. However, closer inspection of Figure 10 reveals the warping of the flow due to the presence of the wall. Even though the influence of the wall is negligible for a single cylinder at G/D = 1 from the wall, the asymmetry of the cylinders' wakes is clear in the present tandem case with G/D = 1 and L/D = 2. The shear layer shed from the bottom half of the cylinder resembles the extended body regime, while the one shed from the top undergoes periodic reattachment. The behaviour of the flow in the small spacing between the cylinders is further discussed in Section 4.3.

Another characteristic of the flow around a single cylinder in the vicinity of the wall, at G/D between 0.25 and 1, is the separation of the downstream wall boundary layer [27, 28]. In the present study, the large L/D allows the wall boundary layer to separate in the wake of both cylinders, with more pronounced recirculation in the wake of the upstream one. On the other hand, the separation of the wall boundary layer occurs only in the wake of the downstream cylinder for L/D = 2. Wang et al. [34] captured the same behaviour experimentally.

Figure 12 represents the instantaneous Q = 10 iso-surfaces for three cases with G/D = 1: a single cylinder in the vicinity of the plane wall (taken from [26]), and tandem circular cylinders with spacing ratios of 2 and 5. At L/D = 2, the wake of the downstream cylinder is turbulent, but does not show signs of large, coherent structures (Figure 12b). Compared to the case of the tandem cylinders in an infinite fluid [52], the wake is narrower and less meandering. This is attributed to the straighter and elongated shear layer shed from the lower half of the cylinder, caused by the presence of the wall.

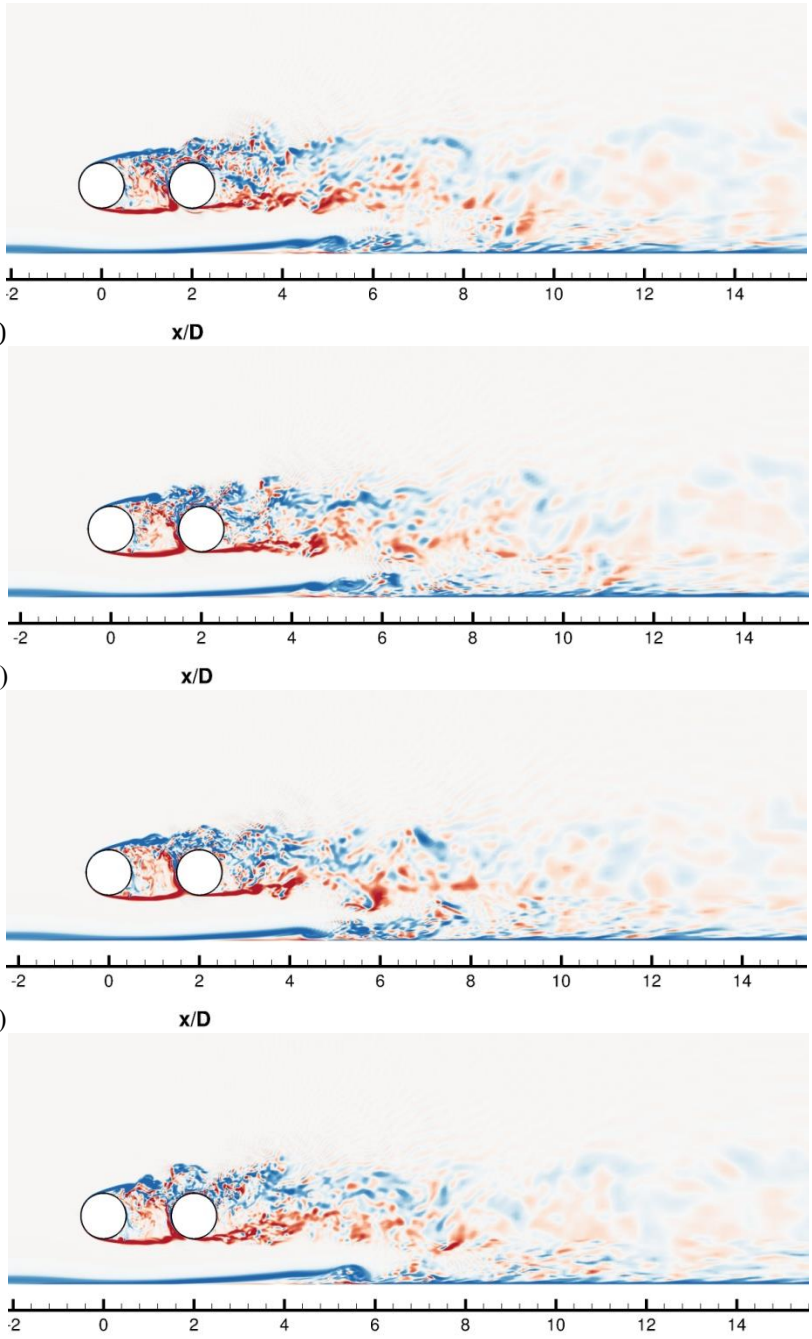

Figure 10. Development of the instantaneous spanwise vorticity (ω_z) through one vortex shedding period at vertical, mid-plane vertical cross-section (z/D = 2). The positive ω_z is presented in red and the negative ω_z in blue colour. G/D = 1, L/D = 2. Figures a to d correspond to t/T = 0, ¼, ½ and ¾, respectively.

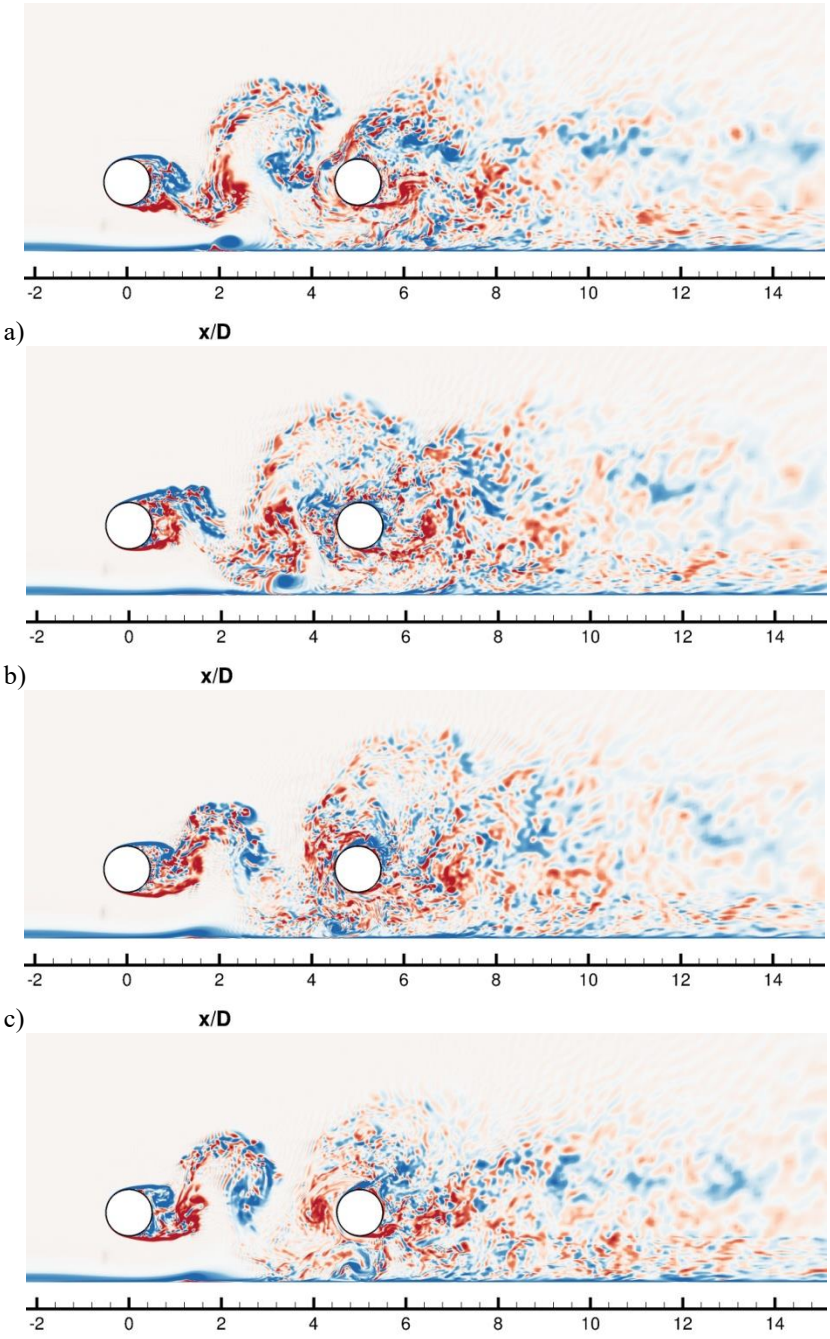

Figure 11. Development of the instantaneous spanwise vorticity (ω_z) through one vortex shedding period at vertical, mid-plane vertical cross-section (z/D = 2). The positive ω_z is presented in red and the negative ω_z in blue colour. G/D = 1, L/D = 5. Figures a to d correspond to t/T = 0, ¼, ½ and ¾, respectively.

Figure 12c also confirms the previously mentioned observation that the presence of the wall deforms the large vortices shed from the upstream cylinder, and thus exposes the downstream cylinder to the asymmetric loads. This further leads to the distortion of the vortices shed from the downstream cylinder. However, similar to the case of one cylinder close to the wall, large periodic structures, interwoven with small vortical structures, are still present in the downstream cylinder wake.

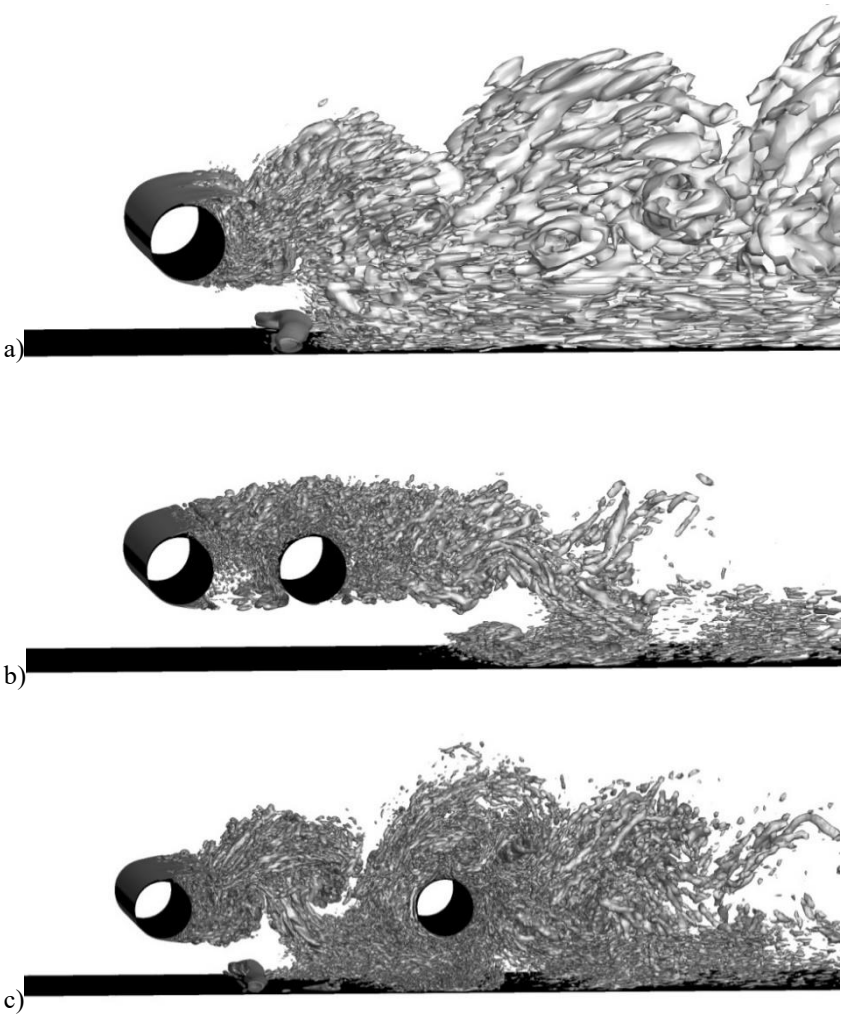

Figure 12. Instantaneous Q = 10 iso-surfaces for G/D = 1.
a) L/D = ∞ (case taken from Abrahamsen Prsic et al. [26]);
b) L/D = 2, case G1 L2;
c) L/D =5, case G1 L5.

The bottom wall boundary layer shedding, identified in Figures 10 and 11, is clearly represented on Figure 12. At G/D = 1, the separation of the wall boundary layer behind the leading cylinder (Figure 12c) develops in the same manner as the one behind a single cylinder at G/D = 1 (Figure 12a). Further downstream, the vortices shed from the upstream cylinder alter the flow in the gap between the downstream cylinder and the wall, resulting in less pronounced and more elongated bottom wall separation. Due to the long, straight shear layer extending across the small spacing, at L/D = 2, the bottom wall boundary layer in the area underneath the cylinders is nearly unaltered. The wake of the downstream cylinder interacts with the bottom wall boundary layer farther downstream than in the case of one cylinder near the wall. Such behaviour is more comparable to a single, elongated body, thus confirming that at L/D = 2, the flow shows characteristics of the extended body regime.

4.3. Influence of the gap

Due to the similarities with the flow around the tandem cylinders in an infinite fluid, the small spacing cases in the present study are classified within the reattachment regime with some features of the extended body regime and the large spacing cases within the co-shedding regime. However, the

presence of the wall alters the flow and yields more specific wake patterns.

Several studies were carried out for the flow around tandem cylinders in an infinite fluid at L/D = 2. The experimental results in [49] pointed to the presence of the symmetric, quasi-static vortices formed between the cylinders. Further investigation by Alam et al. [15] identified the steady reattachment of the shear layers on the downstream cylinders for 1.6 < L/D < 2.3-2.4, while LES simulations by Kitagawa and Ohta [22] showed the symmetric, alternating reattachment for L/D = 2 and Re = 2.2 x 10^4. The symmetric flow between the cylinders was also reported by Palau-Salvador et al. [53], who investigated the flow around two vertical cylinders arranged in a tandem at Re = 1.5 x 10^3. The average streamlines exerted from both the experimental and LES results showed the symmetric vortices between the tandem cylinders.

A different type of flow can be observed in Figure 13, representing the time-averaged streamlines for the two cases with narrow spacing L/D = 2. Due to the strong and steady reattachment of the shear layer shed from the lower half of the cylinder, a steady, large vortical structure is developed over the main part of the area between the cylinders. The vortex occupying the lower half of the spacing in the case of tandem cylinders in an infinite fluid, becomes dominant in the present case, and shows characteristics of the cavity-type flow. The upper side vortex can still be recognised. In the wider gap case, although significantly smaller, the top side vortex is located in front of the upper half of the downstream cylinder, slanting the larger vortex slightly upstream. It manifests as the negative vorticity area in Figure 10. The smaller G/D = 0.6 and the consequent speed-up of the flow in the gap, allow even stronger development of the cavity-flow-like circulation, restricting the top side vortex to a narrow area on top of the spacing between the cylinders.

Based on the PIV measurements at Re = 6.3 x 10^3, Wang et al. [34] proposed a map of flow patterns around the near-wall tandem cylinders. At an intermediate gap (in their definition covering approximately G/D between 0.3 and 1), they indicated the reattachment of the shear layer from the lower half of the cylinder and the asymmetry of the flow in the spacing. However, the experimental results did not give further details of the fine flow structures in the spacing. The previous numerical results are, on the other hand, available only for very low Re. Harichandan and Roy [36], for Re = 200, L/D = 2 and G/D = 0.5, observed a large structure of positive vorticity between the cylinders, similar to Figure 13.

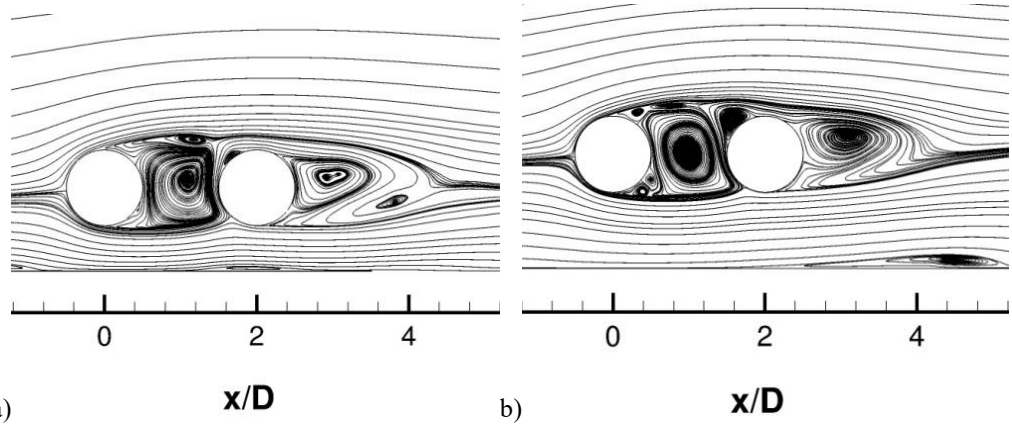

a) b)

Figure 13. Time-averaged flow streamlines at the spanwise mid-section plane (z/D = 2). L/D = 2.
a) G/D = 0.6, case G06 L2;
b) G/D = 1, case G1 L2.

The influence of the plane wall can also be noticed in the wake of the downstream cylinder at L/D = 2. For both the extended body and the reattachment regime, Zdravkovich [10] and Zhou and Yiu [16] report the occurrence of the vortex shedding and the symmetric wake behind the downstream cylinder. In the present case (see Figure 13a and 13b), the wake is elongated and asymmetric. It is significantly longer than the one depicted through the mean streamlines in [53].

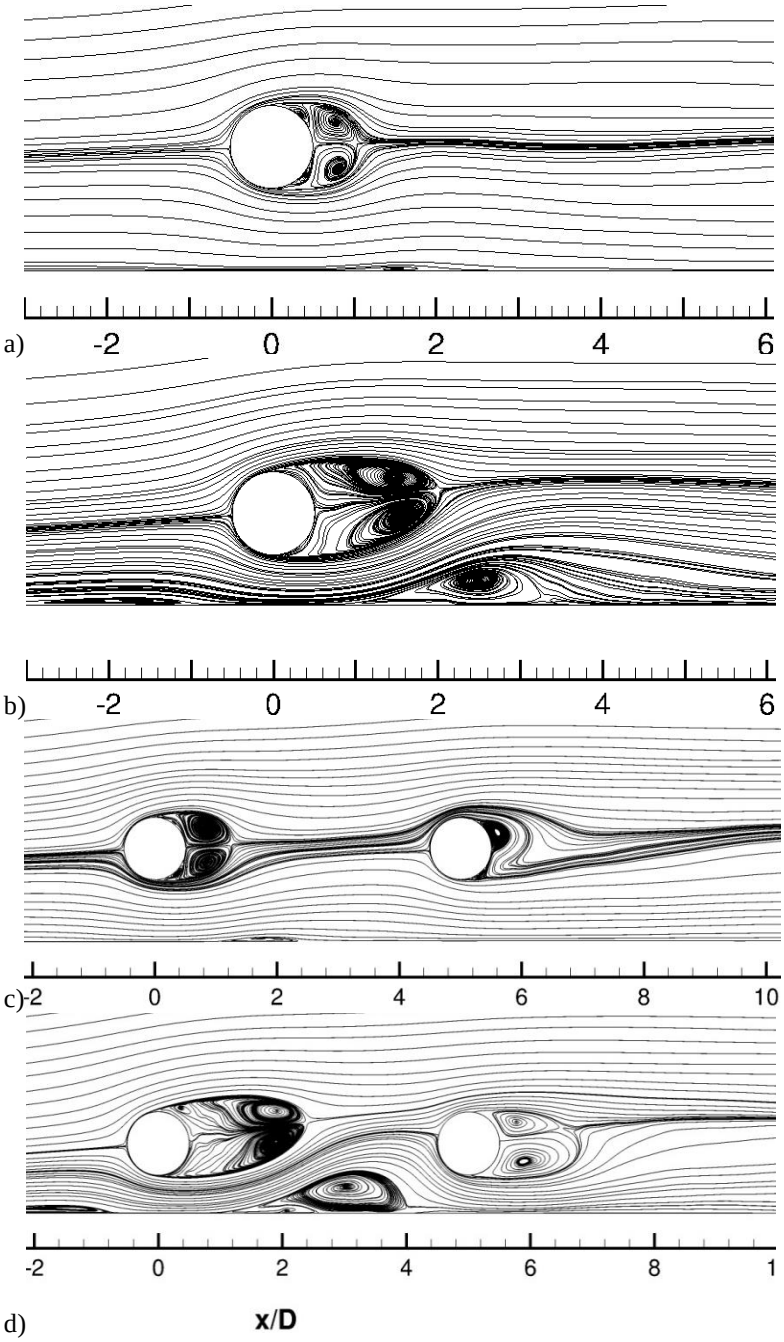

Figure 14. Time-averaged flow streamlines at the spanwise mid-section plane.
a) one cylinder near a plane wall, G/D = 1, from Abrahamsen Prsic et al. [26];
b) one cylinder near a plane wall, G/D = 0.6, from Abrahamsen Prsic et al. [26];
c) L/D = 5, G/D = 1, case G1 L5;
d) L/D = 5, G/D = 0.6, case G06 L5.

Figure 14 presents the comparison of the mean flow streamlines for the cases of one cylinder at G/D= 0.6 and 1 with the cases of tandem cylinders with spacing L/D = 5 and the same G/D. These cases show the development of von Karman vortex shedding in the wake of the upstream cylinder. This behaviour manifests through the time-averaged wake of the upstream cylinder, presented in Figures 14c and 14d, showing large and regular vortices on both sides of the cylinder. The wake flow behind the leading cylinder is comparable to the one around a single cylinder in the vicinity of the wall (Figure 14a and 14b).

In [23], they captured the symmetric mean flow streamlines in the wake of the upstream cylinder of the tandem cylinders in an infinite fluid. Furthermore, they reported that the wake of the downstream cylinder is somewhat shorter than the upstream one, but symmetric and exhibiting the same characteristics as the flow around a single cylinder. In the present study, on the other hand, a strong asymmetry is present in the wake of the downstream cylinder for both gap ratios. As mentioned before, this is attributed to the fact that the impinging vortices, shed from the upstream cylinder, are affected by the presence of the wall.

4.4. Spanwise variation

LES, intrinsically 3D model is chosen for the present study due to its capability of capturing the spanwise variation of the flow. On the other hand, 2D models previously used for the flow around a single cylinder in the vicinity of a plane wall, even though providing good qualitative agreement with the experiments, show significant limitations.

The importance of the three-dimensionality of the flow in the case of one cylinder in a uniform current is investigated in [7], and the case of one cylinder in the vicinity of a plane wall was discussed in [26] while [54] investigated the tandem circular cylinders in an infinite fluid. Preliminary results for tandem cylinders in the vicinity of the wall are published by Abrahamsen Prsic et al. [8]. In the case of a single cylinder in an infinite fluid, Sumer and Fredsøe [1] report that the vortex shedding in the turbulent wake regime is not uniform along the cylinder span, but distributed in long cells. Indications of such cells can be noticed for one cylinder near the wall [26] and for the upstream cylinder in a tandem configuration in the infinite fluid at large spacing ratios ([23], [54]).

Figure 15 shows the spanwise variations of the flow by using the Q-criterion for L/D = 2 and 5 and G/D = 1. Q-criterion depicts the large, coherent vortices and involves the small-scale structures [55]. The near wake of the upstream cylinder at L/D = 5 behave comparable to the single cylinder close to a wall, forming long streamwise varying structures. On the other hand, the small spacing ratio does not allow the streamwise structures to develop, resulting in relatively uniform behaviour of the near wake. This behaviour is in agreement with the conclusions by Wu et al. [54]. Due to the effects of vortex impingement and high turbulence intensity, the coherence in the downstream cylinder wake is not conspicuous.

Observing the Q-criterion in area of the flow separation at the upstream cylinder, uniform and smooth iso-surfaces can be noticed. This is indicating a laminar flow separation, while the transition to turbulence takes place in the near wake. Such flow characteristics are consistent with the subcritical flow regime for the flow around a single circular cylinder [1], where the present results have been classified. Figure 15 shows that the downstream cylinder, for both L/D = 2 and 5, experiences a highly turbulent inflow.

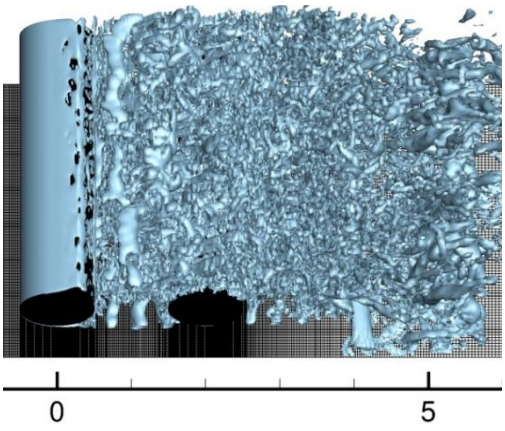

a)

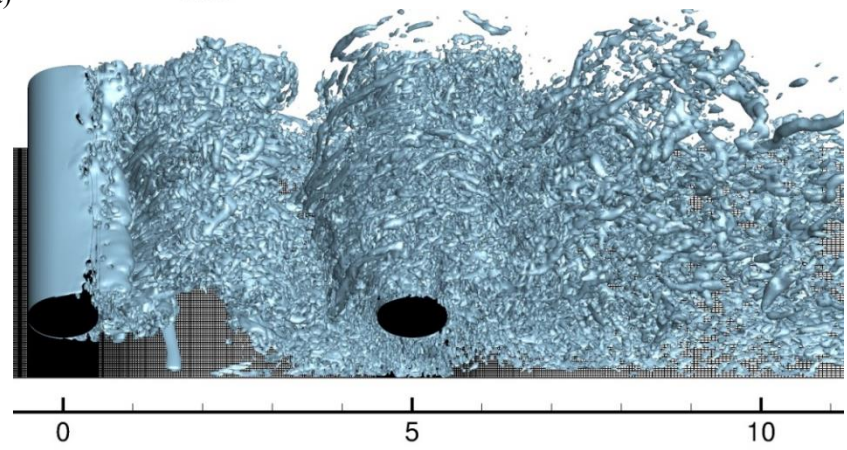

b)

Figure 15. Instantaneous Q = 10 iso-surfaces, viewed from above. G/D = 1.

a) L/D = 2;
b) L/D = 5.

5. Conclusions

Flow around two circular cylinders arranged in tandem configuration and placed in the vicinity of a plane wall is simulated using LES with Smagorinsky subgrid scale model. At Re = 1.31 x 10^4, the influence of the distance between the cylinders, as well as the influence of the plane wall are investigated. The results are presented through the drag and the lift forces exerted on the two cylinders, as well as through the instantaneous and mean flow fields between the cylinders and in the wake of the downstream cylinder. The main conclusions are:

1) For both G/D = 0.6 and 1, the cylinders at L/D = 5 experience the flow behaviour comparable to a co-shedding regime of the tandem cylinders in an infinite fluid. At L/D = 2, the flow is comparable to the reattachment regime with characteristics of the extended body regime.

2) For a large L/D = 5, the flow around the upstream cylinder behaves as the flow around a single cylinder at corresponding G/D. The downstream cylinder at large spacing ratio is, however, influenced by the presence of the wall and the upstream cylinder. It experiences lower $\overline{C_{d2}}$ and yields broader and weaker wake. The main characteristics of the single near-wall cylinder wake at corresponding G/D are still recognizable.

3) The vortices shed from the upstream cylinder at L/D = 5 are distorted by the wall, causing asymmetric impingement on the downstream cylinder. As a consequence, $\overline{C_{d2}}$ oscillates with alternating high and low amplitude.

4) The smaller L/D = 2 suppresses the vortex shedding from the upstream cylinder in a similar manner as for tandem cylinders in an infinite fluid. The downstream cylinder experiences negative $\overline{C_{d2}}$ and sheds an elongated, narrow wake. Due to the presence of the wall, inhibition of the vortex shedding from the downstream cylinder is larger than for tandem cylinders in an infinite fluid. The shear layer from the bottom half of the cylinder exhibits steady reattachment and characteristics of the extended body regime.

5) Even though a single cylinder experiences only slight influence from the wall at G/D = 1, the wall effects on the narrow spaced tandem cylinders are prominent. This is manifested through asymmetric wake of both cylinders and highly altered flow in the spacing between the two cylinders.

6) The wall boundary layer under the cylinders at L/D = 5 experiences vortex shedding under each cylinder in a manner comparable to the single near-wall cylinder case. The narrow spaced tandem cylinders yield bottom wall vortex shedding only in the far wake of the downstream cylinder.

7) Even though the wake of the tandem cylinders is turbulent for all presented combinations of L/D and G/D, the secondary spanwise structures develop only for the L/D = 5 cases.

References

[1] Sumer, B M, Fredsøe, J (2006) Hydrodynamics Around Cylindrical Structures. Revised, reprinted edition. Advanced Series on Ocean Engineering, World Scientific Publishing, Singapore

[2] Zdravkovich, M (1997) Flow Around Circular Cylinders, Vol. 1: Fundamentals. Oxford University Press, Oxford, UK

[3] Thom, A (1928) An investigation of fluid flow in two-dimensions. Aeronautical Research Council, Reports & Memoranda 1194 (Th. Numerical Calc.)

[4] Parnaudeau, P, Carlier, J, Heitz, D, Lamballais, E (2008) Experimental and numerical studies of the flow over a circular cylinder at Reynolds number 3900. Physics of Fluids. 20:085101

[5] Krajnovic, S (2011) Flow around a tall finite cylinder explored by large eddy simulation. Journal of Fluid Mechanics, 676:294-317

[6] Lysenko, D A, Ertesvåg, I E, Rian, K E (2012) Large-eddy simulation of the flow over a circular cylinder at Reynolds number 3900 using the OpenFOAM toolbox. Flow, Turbulence and Combust. 89, 4:491-518

[7] Abrahamsen Prsic, M, Ong, M C, Pettersen, B, Myrhaug, D (2014) Large-eddy simulations of three dimensional flow around a smooth circular cylinder in a uniform current in the subcritical flow regime. Ocean Engineering, 77:61-73

[8] Abrahamsen Prsic, M, Ong, M C, Pettersen, B, Myrhaug, D (2015) Large Eddy Simulations of Flow around Tandem Cylinders Close to a Horizontal Wall. International Journal of Offshore and Polar Engineering 2015; Volum 25, 3:161-169

[9] Tremblay, F, Manhart, M, Friedrich, R (2000) DNS of flow around the circular cylinder at subcritical Reynolds number with Cartesian grids. Proceedings of the 8th European Turbulence Conference, EUROMECH, Barcelona, Spain. 659-662

[10] Zdravkovich, M (1985) Flow induced oscillations of two interfering circular cylinders. Journal of Sound and Vibration, 101, 4:511-521

[11] Zdravkovich, M (1987) The effects of interference between circular cylinders in cross flow. Journal of Fluids and Structures, 1:239-261

[12] Zdravkovich, M M, Pridden, D L (1977) Interference between two circular cylinders; series of unexpected discontinuities. Journal of Industrial Aerodynamics, 2:255-270

[13] Zdravkovich, M M (2009) Flow Around Circular Cylinders, Vol. 2: Applications. Oxford University Press, Oxford, UK

[14] Lin, J C, Yang, Y, Rockwell, D (2002) Flow past two cylinders in tandem: Instantaneous and average flow structure. Journal of Fluids and Structures, 16:1059-1071

[15] Alam, M M, Moriya, M, Takai, K, Sakamoto, H (2003) Fluctuating fluid forces acting on two circular cylinders in tandem arrangement at a subcritical Reynolds number. Journal of Wind Engineering and Industrial Aerodynamics, 91:139-154

[16] Zhou, W, Yiu, M W (2006) Flow structure, momentum and heat transport in a two-tandem-cylinder wake. Journal of Fluid Mechanics, 548:17-48

[17] Song, F-L, Tseng, S-Y, Hsu, S-W, Kuo, C-H (2015) Gap ratio effects on flow characteristics behind side-by-side cylinders of diameter ratio two. Experimental, Thermal and Fluid Science, 66:254-268

[18] Sumner, D (2010) Two circular cylinders in cross-flow: A review. Journal of Fluids and Structures, 26:849-899

[19] Mittal, S, Kumar, V, Raghuvanshi, A (1997) Unsteady incompressible flows past two cylinders in tandem and staggered arrangements. International Journal for Numerical Methods in Fluids, 25:1315- 1344

[20] Meneghini, J R, Saltara, F, Siquiera, C L R, Ferrari Jr., J R (2001) Numerical simulation of flow interference between two circular cylinders in tandem and side-by-side arrangement. Journal of Fluids and Structures, 15:327-350

[21] Bres, G A, Freed, D, Wessels, M, Noelting, S, Perot, F (2012) Flow and noise prediction for the tandem cylinder aeroacoustic benchmark. Physics of Fluids, 24:036101

[22] Kitagawa, T, Ohta, H (2008) Numerical investigation on flow around circular cylinders in tandem arrangement at a subcritical Reynolds number. Journal of fluids and structures, 24:680-699

[23] Uzun, A, Yousuff Hussaini, M (2012) An application of delayed detached eddy simulation to tandem cylinder flow field prediction. Computers and Fluids, 60:71-85

[24] Sainte-Rose, B, Allain, O, Leca, C, Dervieux, A (2014) A study of LES models for the simulation of a turbulent flow around supercritical tandem cylinders. Proceedings of the ASME 2014 33rd International Conference on Ocean, Offshore and Arctic Engineering OMAE2014-24031.

[25] Duchaine, F, Boileau, M, Sommerer, Y, Poinsot, T (2014) Large Eddy Simulation of flow and heat transfer around two square cylinders in a tandem arrangement. Journal of Heat Transfer, 136:101702

[26] Abrahamsen Prsic, M, Ong, M C, Pettersen, B, Myrhaug, D (2016) Large Eddy Simulations of

Flow around a Circular Cylinder close to a Flat Seabed. Marine Structures, 46, 127-148

[27] Price, S J, Sumner, D, Smith, J G, Leong, K, Paidoussis, M P (2002) Flow visualization around a circular cylinder near to a plane wall. Journal of Fluids and Structures, 16, 2:175-191

[28] Alper Oner, A, Salih Kirgoz, M, Sami Akoz, M (2008) Interaction of a current with a circular cylinder near a rigid bed. Ocean Engineering, 35:1492-1504

[29] Wang, X K, Tan, S K (2008) Comparison of flow patterns in the near wake of a circular cylinder and a square cylinder placed near a plane wall. Ocean Engineering, 35:458-472

[30] Brørs, B (1999) Numerical modelling of flow and scour at pipelines. Journal of Hydraulic Engineering, 125, 5:511-523

[31] Zhao, M, Cheng, L, Teng, B (2007) Numerical modelling of flow and hydrodynamic forces around a piggyback pipeline near the seabed. Journal of Waterway, Port, Coastal and Ocean Engineering, 133, 4:286-295

[32] Ong, M C, Utnes, T, Holmedal, L E, Myrhaug, D, Pettersen, B (2010) Numerical simulation of flow around a circular cylinder close to a flat seabed at high Reynolds numbers using a k- ε model. Coastal Engineering, 57, 10:931-947

[33] Sarkar, S, Sarkar, S (2010) Vortex dynamics of a cylinder wake in proximity to a wall. Journal of Fluids and Structures, 26:19-40

[34] Wang, X K, Zhang, J-X, Hao, Z, Zhou, B, Tan, S K (2015) Influence of wall proximity on flow around two tandem circular cylinders. Ocean Engineering, 94:36-50

[35] Bhattacharyya, S, Dhinakaran, S (2008) Vortex shedding in shear flow past tandem square cylinders in the vicinity of a plane wall. Journal of Fluids and Structures, 24:400-417

[36] Harichandan, A B, Roy, B (2012) Numerical investigation of flow past single and tandem cylindrical bodies in the vicinity of a plane wall. Journal of Fluids and Structures, 33:19-43

[37] Zhao, M, Vaidya, S, Zhang, Q, Cheng, L (2015) Local scour around two pipelines in tandem in steady current. Coastal Engineering, 98, 1-15

[38] Li, Z, Abrahamsen Prsic, M, Ong, M C, Khoo, B C (2018) Large Eddy Simulations of flow around two circular cylinders in tandem in the vicinity of a plane wall at small gap ratios. Journal of Fluids and Structures, 76:251-271

[39] Knight, P J, Wilkinson, M, Glorioso, P (1993) Current profile and sea-bed pressure and temperature records from the northern North Sea. Challenger Cruises 84 and 85. September 1991 - November 1991. Birkenhead, Proudman Oceanographic Laboratory, Report No. 28, 417pp

[40] Det Norske Veritas as. Offshore standard Dnv-Os-F101; submarine pipeline systems. Det Norske Veritas, August 2012

[41] Prsic, M, Ong, M C, Pettersen, B, Myrhaug, D (2012) Large eddy simulations of three-dimensional flow around a pipeline in a uniform current. Proceedings of the 31st International Conference on Ocean, Offshore and Arctic Engineering OMAE2012-83144

[42] Smagorinsky, J (1963) General circulation experiments with the primitive equations. Monthly Weather Review, 91, 3:99-164

[43] Breuer, M (1998) Large eddy simulation of the subcritical flow past a circular cylinder: numerical and modeling aspects. International Journal for Numerical Methods in Fluids, 28:1280-1302

[44] Breuer, M (2000) A challenging case for large eddy simulation of high Reynolds number circular cylinder flow. International Journal of Heat and Fluid Flow, 21:648-654

[45] Ferziger, J H, Peric, M (2001) Computational methods for fluid dynamics. 3rd Ed, Springer-Verlag, Berlin, Germany

[46] Bearman, P W, Zdravkovich, M M (1978) Flow around a circular cylinder near a plane boundary. Journal of Fluid Mechanics, 89:33-47

[47] Lei, C, Cheng, L, Kavanagh, K (1999) Re-examination of the effect of a plane boundary on force and vortex shedding of a circular cylinder. Journal of Wind Engineering and Industrial Aerodynamics, 80:263-286

[48] Ljungkrona, L, Norberg, C H, Sunden, B (1991) Free-stream turbulence and tube spacing effects on surface pressure fluctuations for two tubes in an in-line arrangement. Journal of Fluids and Structures, 5:701-727

[49] Igarashi, T (1981) Characteristics of the flow around two circular cylinders arranged in tandem (1st report) Bulletin of the JSME, 24:232-331

[50] Alam, M, Zhou,Y (2007) Phase lag between vortex shedding from two tandem bluff bodies. Journal of Fluids and Structures, 23:339-347

[51] Mathieu, J, Scott, J (2000) An Introduction to Turbulent Flow. Cambridge University Press, Cambridge, UK

[52] Ljungkrona, L, Sunden, B (1993) Flow visualization and surface pressure measurement on two tubes in an inline arrangement. Experimental Thermal and Fluid Science, 6:15-27

[53] Palau-Salvador, G, Stoesser, T, Rodi, W (2008) LES of the flow around two cylinders in tandem.

Journal of Fluids and Structures, 24:1304-1312
[54] Wu, J, Welch, L W, Welsh, M C, Sheridan, J, Walker, G J (1994) Spanwise wake structures of a circular cylinder and two circular cylinders in tandem. Experimental Thermal and Fluid Science, 9:299-308
[55] Lesieur, M, Metais, O, Comte, P (2005) Large-Eddy Simulations of Turbulence. Cambridge University Press, New York, USA